



HAL
open science

3D Reconstruction and Geostatic Analysis of an Early Medieval Cemetery (Olonne-sur-Mer, France)

Rozenn Colleter, Jean-Baptiste Barreau

► **To cite this version:**

Rozenn Colleter, Jean-Baptiste Barreau. 3D Reconstruction and Geostatic Analysis of an Early Medieval Cemetery (Olonne-sur-Mer, France). *Remote Sensing*, 2021, 13 (9), pp.1688. 10.3390/rs13091688 . hal-03212300

HAL Id: hal-03212300

<https://univ-rennes.hal.science/hal-03212300>

Submitted on 26 May 2021

HAL is a multi-disciplinary open access archive for the deposit and dissemination of scientific research documents, whether they are published or not. The documents may come from teaching and research institutions in France or abroad, or from public or private research centers.

L'archive ouverte pluridisciplinaire **HAL**, est destinée au dépôt et à la diffusion de documents scientifiques de niveau recherche, publiés ou non, émanant des établissements d'enseignement et de recherche français ou étrangers, des laboratoires publics ou privés.



Distributed under a Creative Commons Attribution 4.0 International License



Article

3D Reconstruction and Geostatic Analysis of an Early Medieval Cemetery (Olonne-sur-Mer, France)

Rozenn Colleter ^{1,2,*} and Jean-Baptiste Barreau ³

¹ French National Institute for Preventive Archaeological Research (INRAP), 37 rue du Bignon, 35577 Cesson-Sévigné, France

² Centre for Anthropobiology and Genomics of Toulouse (CAGT), Forensic Sciences and the Study of Image Libraries (Team FOSSIL), CNRS, UMR 5288, Faculté de Médecine Purpan, University of Toulouse, Bat A37 Allées Jules Guesde, 31000 Toulouse, France

³ CReAAH, CNRS, University of Rennes, UMR 6566, Campus de Beaulieu Bât24 RDC P009, Avenue du Général Leclerc, 35000 Rennes, France; jean-baptiste.barreau@univ-rennes1.fr

* Correspondence: rozenn.colleter@inrap.fr

Abstract: A preventive excavation performed in 2018 prior to development work led to the discovery of more than 213 subjects buried from the 4th to the 11th centuries in the 1850 m² dug area. This is a cemetery located in Olonne-sur-Mer in France (46.53723, −1.77603). The complex is limited to the south by a ditch. To the north, no limits were observed during the excavation and, to the west, ancient archaeological surveys suggest an extension of the burial area. Biological analysis of the skeletons reveals a demographic characterizing a natural community, with an under-representation of children under 5 and with subjects under 20 appearing to be grouped together in the center of the area. The place where the youngest are buried often testifies to a strategic position in Christian contexts (near church doors, under *sub stillicidio* gutters, etc.). Funeral practices are characterized by numerous skeletal alterations, especially in the western area of the site where their concentrations are particularly significant. These are not ossuaries but rather supernumerary bones present in the fills of graves of subjects in place or old tombs where no skeletons in place are preserved. These alterations mark the areas where burials are most frequent. The 3D reconstruction is coupled with geostatistical analyses (heatmap and Moran's index), considering the digging of the land, the concentration of residual artefacts found in the graves, but also the biological characteristics of the sample and the funeral practices uncovered. From 2D entities generated with GIS software, the process of the elevation and sculpture of the volumes is innovative, because even if it is carried out by precise but classical computer graphics techniques, it is led by advanced taphonomical and anthropological reflections. This makes it possible to propose empty spaces, a potential gathering area for the village community and circulation paths. These elements are essential in order to go beyond the storytelling often proposed in archaeology and propose a vision based on the coherence of the observed facts. Even when the archaeological remains are only sunken (no preserved elevation), the integration of multisource archaeological data (biological anthropology, funerary, artefacts and pit size) allows relevant 3D reconstructions as a formidable tool for discussing past occupations. Three-dimensional technologies make it possible to recreate a lost environment to allow a better understanding of the site. They are didactic and help to share data between researchers and/or the public, especially when they are invisible such as the presence of empty space.

Keywords: archaeology; anthropobiology; cemetery; grave; 3D reconstructions; GIS; DTM; early medieval



Citation: Colleter, R.; Barreau, J.-B. 3D Reconstruction and Geostatic Analysis of an Early Medieval Cemetery (Olonne-sur-Mer, France). *Remote Sens.* **2021**, *13*, 1688. <https://doi.org/10.3390/rs13091688>

Academic Editor: Sara Gonizzi Barsanti

Received: 8 March 2021
Accepted: 23 April 2021
Published: 27 April 2021

Publisher's Note: MDPI stays neutral with regard to jurisdictional claims in published maps and institutional affiliations.



Copyright: © 2021 by the authors. Licensee MDPI, Basel, Switzerland. This article is an open access article distributed under the terms and conditions of the Creative Commons Attribution (CC BY) license (<https://creativecommons.org/licenses/by/4.0/>).

1. Introduction

Many major archaeological discoveries are now made using digital terrain models (DTMs), often based on surveys derived from LiDAR scans that allow the observation of remains hidden under dense vegetation [1,2]. This work generally covers large areas

and allows a proper diagnosis of monumental remains, as the identification of small structures [3], or even hollow structures, can be problematic. These approaches are interesting in areas that are difficult to access and with a high forest cover, such as the Mayan rainforests [4] or the mountains of China [5]. Archaeology also exploits images taken from aircraft for decades, or more recently from drones, to detect buried structures [6,7]. At the scale of preventive archaeological excavations, limited to land development projects, the range of remote sensing methods is mainly based on topographic surveys of structures to create DTMs with databases and GIS. These analysis tools are powerful, but still little used, especially for the 3D reconstruction of burial sites.

The study of ancient cemeteries and the problematics associated have considerably evolved over the last few decades. In the 19th century and until the development of biological anthropology and the archeological sciences, it was mainly the small finds that were coveted [8,9]. The human skeletons thus occupied only a marginal place in the research, there were little or no studies. We had to wait until the development of anthropological biometric techniques and the appearance of radiocarbon dating from bones during the 1950s [10] that the human remains could really be considered as a source of information. Today, aiming for a “total archaeology”, the studies are at times, based on in depth biological research (characterization of samples, recruitment, DNA, isotopes, forensics, pathology, etc.) [11–14], a funerary archaeology, which is very descriptive about the tomb to reconstituted funeral practices [15–18] and the precise analysis of contexts, sediments and associated artefacts [19–22]. The objectives cover the reconstitution of past populations (diets, mortality and morbidity, relatives, migration, etc.) and their beliefs (notably by the study of the diversity of their funeral practices) [23]. Despite the new cyber tools, which are available to archaeologists and anthropologists, the general environment of cemeteries and burial grounds are often found to be neglected and the contexts are sometimes forgotten about in the framework of large surveys due to the change of the scales made (i.e., look at the studies at the continental scale on DNA, which are not always applied to the context of tombs [24,25]). Bearing in mind, at the local analysis of a cemetery, the spatial elements could lead us to the social status of the dead according to the emplacement of the tomb [26–28]. Effectively and notably in Christianity contexts, the position of the tomb is not by hazard [28–30]. The study of a DTM with archaeological and anthropological databases is an interesting perspective for discussing the installation of cemeteries, notably by the observation of empty spaces.

Based on a recent rescue archaeological excavation, we propose to link the biological and funerary information with the spatial environment to reconstitute the invisible and propose a spatial interpretation from information based on analytical techniques. We propose notably to observe the MNI (minimum number of individuals) by tomb, in the primary position and secondary to evaluate the places the most sought after, with a more important breakdown. In confronting the biological results geolocated on the DTM, we observe the spaces reserved for certain biological characteristics (age at death). From the elements of residual artifacts, we can determine the places most visited by the living, the passage ways. The creation of a 3D environment coupled to a database allow the researcher to propose the hypothesis for which geostatistical analysis allows one to release the facts and numerical trends. Beyond the simple description of the remains, the 3D reconstitution of the invisible allows the proposal of pertinent and measurable hypotheses, for the installation of a funerary ensemble of the early Middle Ages because no cemetery installs or grows by hazard [31].

2. Materials and Methods

2.1. Description of the Site

A rescue excavation before the proposed construction work at 14 Rue de la Paix, Olonne-sur-Mer (west of France) revealed a part of a funerary space dating to the Early Middle Ages with a surface of about 1850 m² (Figure 1A,B) [32]. Given the context of preventive archaeology and the limited time available for excavations, we did not have

the entire cemetery, nor its limits, but still a good and sufficiently representative sample. Distributed into 174 sepulchral pits were 213 subjects, 165 adults and 48 children were buried on the site during 6 centuries (from the 5th century until the 10th century) of which 140 were in their primary position, which is to say their bodies had decomposed where the archaeologist found them. No multiple simultaneous deposit was observed, the tombs were all strictly individual even if 73 individuals come from secondary burials characterized by the body then the skeleton being deposited at several times and places [15]. The incomplete character of the remains of bones indicates the dismantling of tombs and the manipulation of bones, without doubt related to the management of the funerary area throughout time [33]. There were only inhumations, no cremations were found, which conforms to the Christian rituals used in Gaul since the early Middle Ages [34]. The tombs are limited, in the south by a ditch, with several sepulchral pits taking the same orientation, but without any intercutting, despite the dense concentration of tombs, which may well suggest that they were contemporary (Figure 1C).

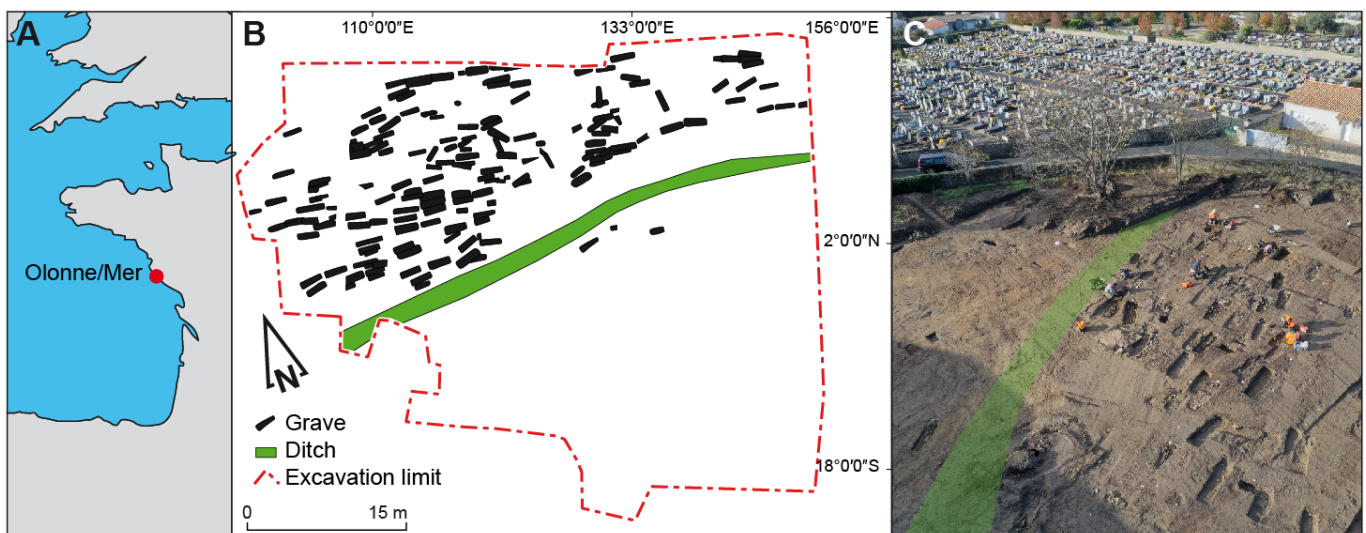


Figure 1. (A) Location of the French city of Olonne-sur-Mer; (B) Location of the graves and the ditch at the south; (C) Drone photography of the digging site.

2.2. Anthropological Methods

The method used for excavation and the lifting of the skeletons is classic, putting into operation the techniques that have been developed over the past twenty years in archaeo-anthropology [35,36]. Three survey (topographical) points were systematically recorded on the body, skull, pelvis, and ankles, to see the general altitude of the inhumation, the orientation of the body and to georeference the skeleton. The contour of the sepulchral pit is also surveyed. The excavation of sepulchral ensembles implies the treatment of numerous details for the study of each burial (archaeology, taphonomy and biology). For the efficient recording and exploitation of the results, the information was recorded on a database management system (DBMS) called HumanOS, for storing, the recording, modification, sorting and interrogating the information [37]. The input of the data is also more secure, minimizing the risk of error (entry constraints). The elaboration of the anthropological database is coupled with the georeferencing of the primary individuals for spatial queries. The exports that may be generated by this database concerns, the catalogue of the tombs, the skeletons (vectorized format) or the tables (csv format) allowing to easily import the data to a geographic information system like QGIS.

The determination of funeral practices is based on archaeo-thanatological observations in the field [38]. The preservation or not of all anatomical connections, the observation of any preserved volumes, the unstable balances or linear effects on human skeletons,

all provide information about the burial method and funeral architecture. Age at death was estimated for adults from observations of the sacropelvic surface [39], completed by the evaluation of the degree of dental wear, an indicator that seems quite pertinent at a population level according to Owen and Lovejoy [40,41]. For the adolescents and children, the age at death was mainly attributed by the observation of the stages of dental mineralization [42,43]. When this was impossible (absence of observation and teeth included) the diaphasia length of long bones or the maturation stage of the bones was used depending on the estimated age of the dead [44–49].

2.3. Statistics

To assess the degree of chance in the spatial distribution of graves and to highlight significant neighbor-to-neighbor relationships with the rest of the group, systematic exploratory mapping analyses were conducted. From a statistical point of view, the process is based on the assumption of independence between variables. Thus, if a variable is spatially self-correlated, the independence hypothesis (H0) is not respected (random dispersion). Geostatistical processing can then spatially quantify the data to support interpretations and usefully complements simple graphic representations.

The Moran's index (Moran's I) was chosen for its robustness and is defined as the ratio of covariance to variance [50,51]. The calculations were made with the R "ape" package [52]. By default, the index determines that the higher the neighbor number, the more weight the individual has in the weight matrix. A distance between these neighbors can be defined to influence the covariance of this point and its neighbors in relation to the variance of all points. The result of the calculation of Moran's I is interpreted as a correlation coefficient, ranging from -1 (negative spatial self-correlation: negative association, avoidance and repulsion) to 1 (positive spatial self-correlation involving notions of aggregation and attraction), the zero-value marking the absence of spatial self-correlation (random distribution). The value of the Moran's index can then be interpreted as part of the variance explicable by the neighborhood, so a Moran's I with $I = 0.25$ would attribute 25% of the variance to the values in the neighborhood. Combined with this index, p -value (p) indicates the significance of self-correlation.

To complete these indices and obtain a spatialized reading of statistical results, choropleth heatmap maps were generated with QGIS.

2.4. Creation of Successive DTM

2.4.1. The "Bottom of Form" DTM

As this was a rescue excavation with a limited budget and timeframe, no UAV or LiDAR surveys were performed. However, some topographic points were surveyed with a tacheometer and, given the scientific interest, we nevertheless wished to create DTMs that could bring knowledge to archaeological reasoning, even if their resolution could be improved by the use of dedicated technologies. Three DTM were built from the many topographical points survey in the field and data from Geoportail. The distribution statistics according to these two methods are summarized in Table 1.

Table 1. Results of the nearest neighbor analysis algorithm obtained with QGIS [53].

Acquisition Method	Observed Mean Distance	Expected Mean Distance	Nearest Neighbour Index	Number of Points	Z-Score
Topographic points	0.246	0.474	0.519	3684	−55.803
Geoportail	7.367	0	142,943.904	42	1,772,222.02

The first DTM presents the "bottom of form", the second, the "surface" of the archaeological field before stripping and the last restores the ground level in the early Middle Ages (the "funeral mound" DTM). The first was created from the survey points in the field and using the QGIS 3.16.1-Hannover software (Figure 2A). A black and white raster illustrates

the elevations from the TIN interpolation method (Figure 2B), and then the 3D model is created with the DTM to3D plugin [54] (Figure 2C).

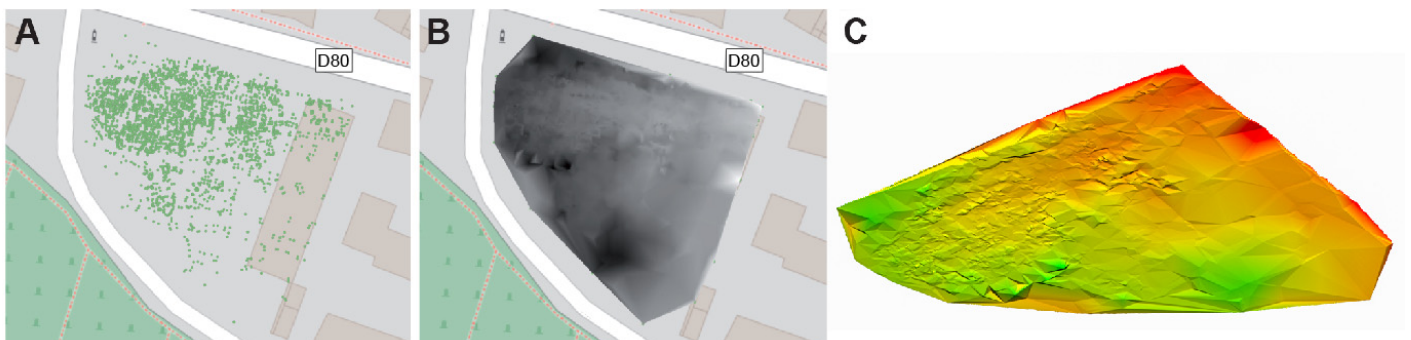


Figure 2. Process of creating the numerical “bottom of form” field model from survey points. (A) survey point recorded in the field; (B) raster generated from survey points; (C) 3D model.

Once integrated into the 3dsmax software, the mesh was smoothed with the TurboSmooth modifier, implementing the Catmull–Clark algorithm [55]. The reconstruction of the tombs was carried out by following 4 steps (Figure 3A–D). (i) Cutting an area encompassing the vicinity of the burial and detachment from that area of the main mesh. (ii) Extrusion of the shape of the burial, directed downwards and expected to pass entirely below the surface of the DTM cutout. The depth is determined using the values shown in Table A1 in Appendix A. (iii) Application of the ProBoolean modifier [56] with subtraction operation to dig the grave. In case of overlapping excavations, we also applied a ProBoolean modifier with overprint option to delineate the bottoms limits. (iv) Application of the Chanfrein modifier [57] on the edges bordering the bottom and upper edges, to smooth out them, and then attached to the main mesh (Figure 3E).

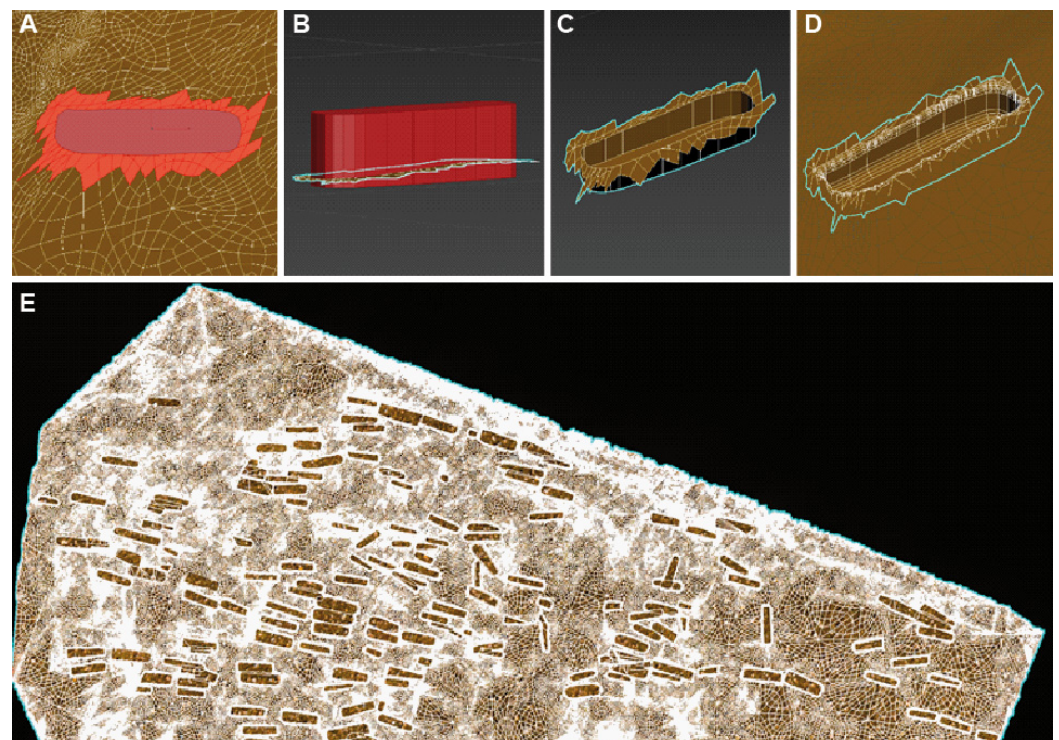


Figure 3. (A–D) Four steps in the process of rebuilding a grave; (E) Wired mesh of the “bottom of form” with the tombs north of the embankment.

The generation of rigged virtual humans is now relatively easy due to open-source software like MakeHuman [58]. With this software, we generated a generic 3D mannequin, whose rigging allows its easy positioning from the survey points recorded under the skull, pelvis and between the ankles. Obtaining the precise depths of tombs is deduced from this same information (Figure 4A,B). These points were addressed with the point cloud object module, which is directly integrated into the 3dsmax software. This same software also allows the rapid generation of stylized views such as “ink”, allowing the enhancement of the contours, and thus an easy reading of the geometries (Figure 4C). Some burials around an empty space had already been processed with Virtualanthropy [59] software, which allowed us to 3D position photos taken on site. The set fits correctly into the overall scene (Figure 4D,E).

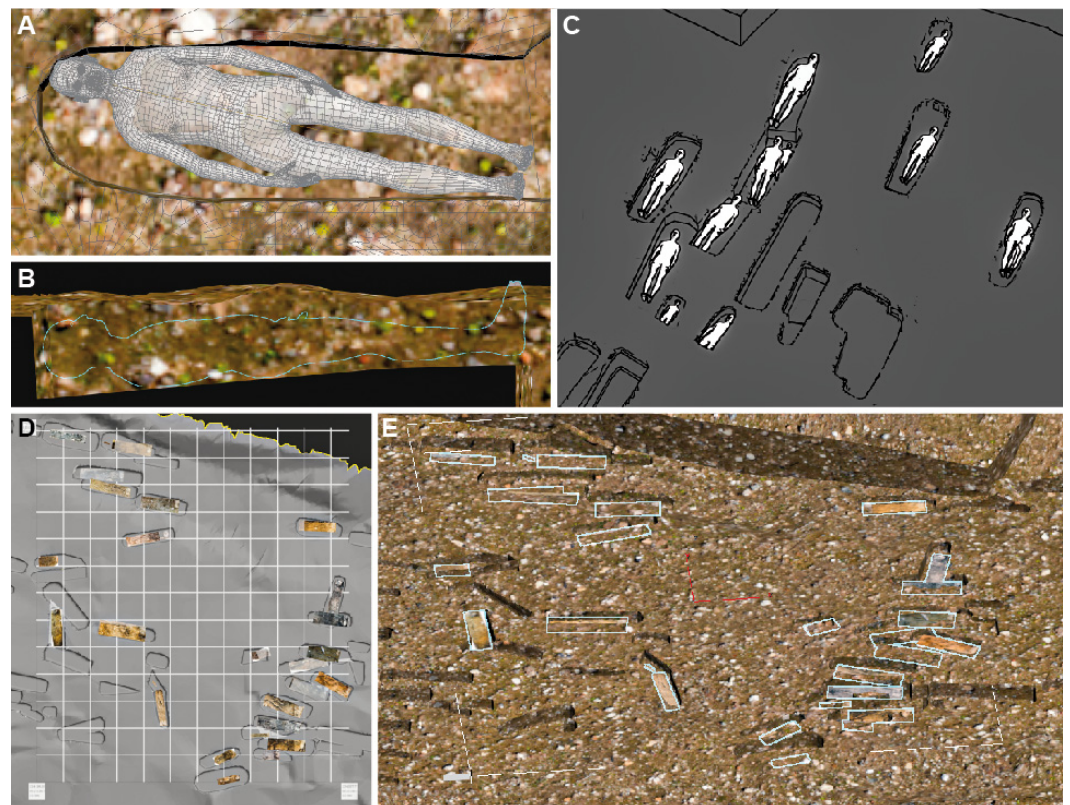


Figure 4. (A,B) A dummy’s head-to-head positioning process in burial 114 to position the bottom more precisely; (C) Stylized 3D view of the same process in progress on burials 104, 105, 110, 114, 115, 122, 123, 125, 126, 136, 170 and 174; (D,E) Integrating photos taken on-site with Virtualanthropy software.

2.4.2. The “Surface” DTM

A second DTM was built, it restored the stripped topsoil and archaeological sediments filling the burial pits and archaeological features. The surface level was restored from Geoportail’s survey points (Figure 5A). This “surface” DTM provides more accurate topographical information than the NGF information (French spot heights) from Geoportail and shows a flat area with a very slight dip from the terrain to the west. This DTM could also accurately calculate the volume of soil impacted by each archaeological structure from the soil trodden by past populations since no geomorphological changes were recorded (Figure 5B).

2.4.3. The “Funeral Mound” DTM

The last DTM restores the topography of the soil at the time of its burial occupation. Without descriptive information of surface development due to soil erosion and successive

post-cemetery occupations on this plot, we based this restitution on the assumption that the volumes of excavated soil are left more or less in place. In the absence of suitable mechanical means for the early Middle Ages, the parsimony leads researchers to base their reasoning on the simplest patterns, namely here the constitution of a mound above the funerary features. The DTM then takes into account both the volume of land excavated (V_0) (subsoil and topsoil) and the bulking factor (V_b). When the soil is disturbed due to the excavation of a sepulchral pit or the digging of a ditch, the removed soil grows in volume. An excavated cubic meter never results in a cubic meter of discharged soil and depending on the soil types and humidity, the multiplication is more or less strong: a sandy earth, for example, produces less volume than a marly soil [60,61]. In Olonne-sur-Mer, the fills of the sepulchral pits are characterized by a clayey-sandy sediment, even silty in the lowest topographic areas. It is a mixture of small rocks linked to the degradation of geological substrates (here metarhyolite [54]) with topsoil covering the structures. Anthropogenic limestone blocks also sometimes dot the fills, the ultimate remnants of ancient forms of tombs and/or the presence of stone in the tumular mound. Based on these elements, we considered for this soil a bulking factor (k) of 1.25.

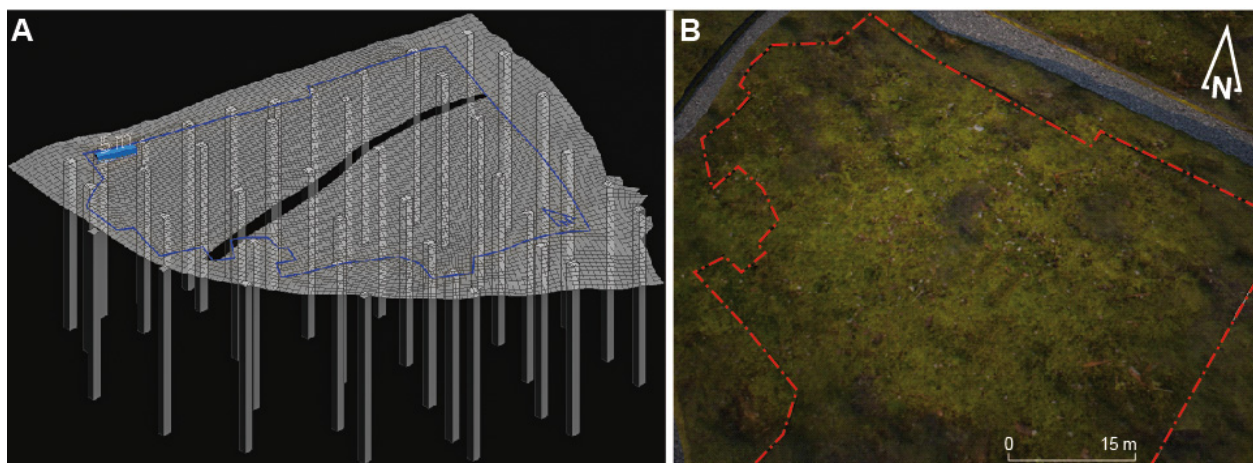


Figure 5. (A) Creating the surface DTM from Geoportail data; (B) rendering a 3D topographical framework of the site prior to the excavation.

$$V_b = V_0 * k \quad (1)$$

(V_b : bulking volume; V_0 : compacted volume in situ; k : bulking factor).

In addition to the bulking volume, the burial mound (V_m) must also take into account the empty spaces of the tomb created by the containers (coffin, sarcophagus and encasing of the pits) and/or the volume of the body deposited before its decomposition (V_c). Depending on the determination of the funerary architectures and the size of the tomb, the volume of the container is then between 0.068 (small child's grave) and 0.78 m³ (large square pit) (Appendix A, Table A1). A minimum and arbitrary height of 40 cm for these structures was applied for the calculation. In the absence of a container, voids observed around the body during excavation and the interpretation of the deposit of the corpse directly into the pit, a volume of 0.075 m³ for adults and 0.037 m³ for children was arbitrarily applied corresponding to body volume. From these calculations, the mounds can then be easily restored and the monumentality of the tombs brought back.

The volume of the mounds was therefore calculated according to the following formula:

$$V_m = V_b + V_c \quad (2)$$

(V_m : volume of the mound; V_b : bulked volume; V_c : volume of the container/body).

The ditch modeling was carried out by initially extruding the 3 vertical sections along its 2D surface originally drawn under QGIS. Due to the new integrations of recent retopology algorithms into the 3dsmax software, we applied the Quadriflow algorithm [62] to the resulting volume to make it clean, easy to use and obtain a relevant estimate of 115.23 m³. Given the complexity of the mesh of the “bottom of form” terrain, the Boolean operation of digging like those of the tombs could not be carried out. Hand-cutting of the 2D surface on the “bottom of form” mesh and a union with the bottom of the extruded volume of the ditch content resulted in a satisfactory result (Figure 6A). The embankment to the south was restored from the strata of the ditch fill and the observation of the presence of an empty space 3–4 m wide immediately north of this structure, the last vestige of a possible embankment in the cemetery. The ditch has a rounded to ‘V’ profile, with a maximum width of 2 m and a depth of 50 cm. It crosses the entire site from east to west, in the direction of the slope, for nearly 49 m. Several stratigraphic units make up the fill, betraying regular maintenance of the sides. Traces of waterlogging (ferro-manganic concretions, white marbled orange coloration, etc.) indicate a rather open, collector-type operation, probably to collect water (Figure 6B). The reconstruction of the edge embankment was carried out with an extrusion of its 2D limits, also originally drawn under QGIS, which then underwent a “turbosmooth” shaking and smoothing. Its volume from $115.23 \times 1.25 = 144.04 \text{ m}^3$ was obtained geometrically by adjusting its vertical scale to obtain the correct value indicated by the 3dsmax measure utility (Figure 6B).

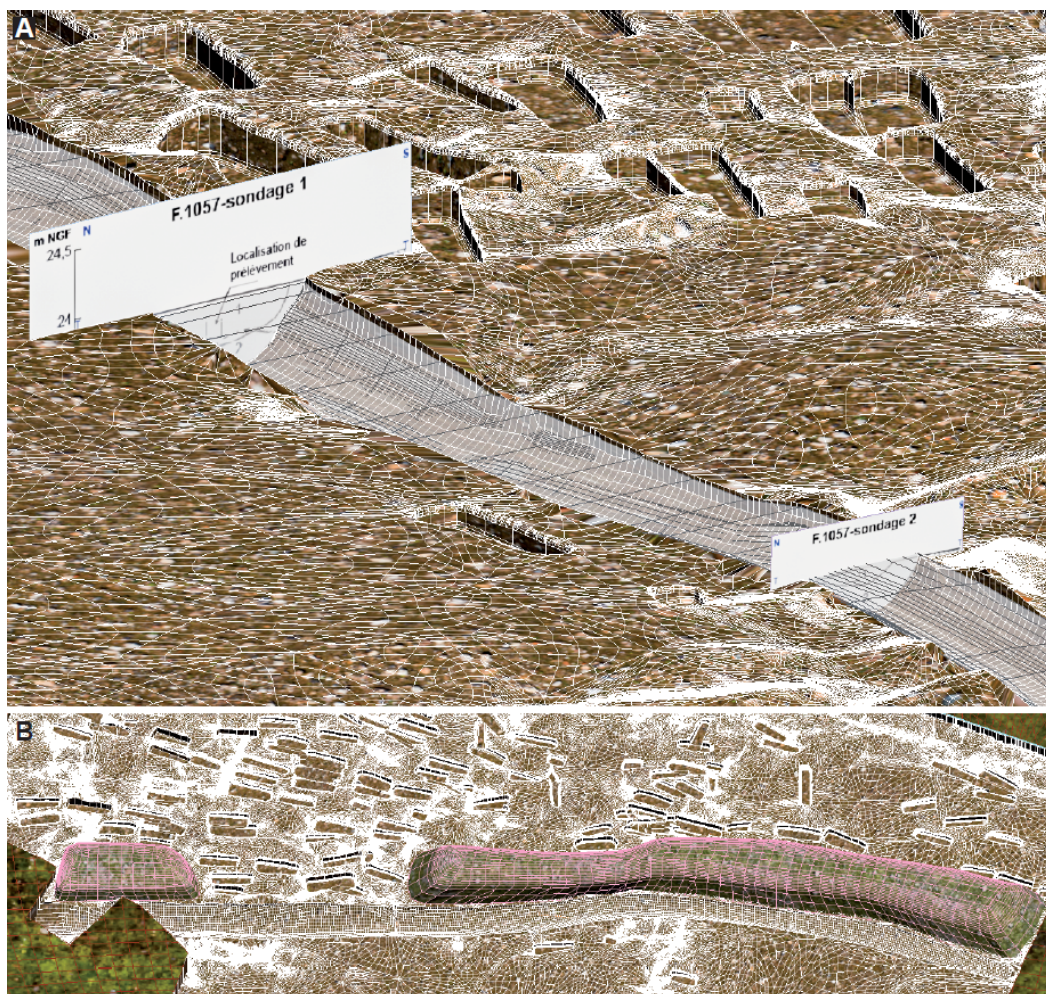


Figure 6. 3dsmax viewport showing the reconstruction of the border embankment. (A) digging the edge ditch on the mesh; (B) return of the volume of the ditch.

The 3D reconstruction of the mounds was the most time-consuming step of this work because its automation was too complex to implement due to the variety of forms of the tombs. For each of the 174 polygons illustrating the contours of the graves, we extruded them downwards to the minimum altitude of the corresponding head-basin-foot points (Figure 7A). We then retopologized these same contours by applying the Quadriflow algorithm [63] to mesh them strongly. We then selected a longitudinal slice of vertex with the soft selection tool [64] to bulge the shape. This slice selection had to be made visually to best match the shape of the graves. To obtain a closed volume, we used the “cap” tool [65] on the lower edge, flattened the resulting face with the “make planar” tool along Z and lowered this polygon to the minimum altitude of the border (Figure 7B). Finally, we rescaled this mesh resulting along Z, so that its volume corresponds to that calculated theoretically by the formula mentioned above.

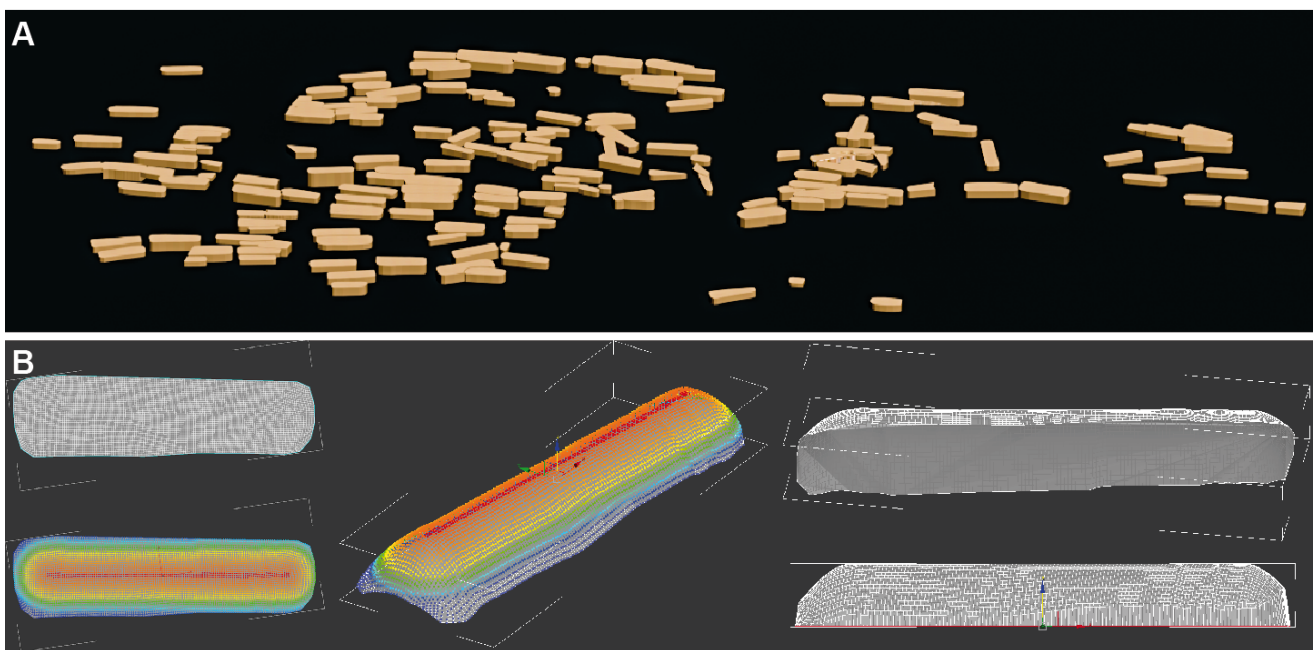


Figure 7. (A) Reconstruction of pit volumes; (B) steps in the process of reconstructing the mounds.

2.5. Data and Geostatic Confrontation

The creation of 3D heatmaps was done by finely retopologizing [63] a plane (Figure 8A), then applying a displace modifier (Figure 8C) [56] from a black and white image produced by QGIS with an outline for recalibration on site (Figure 8B). Extensive scaling was done to clearly distinguish the concentrations, including the lowest. The heights thus represent only a concentration level based on the highest and lowest. This volumetric representation has the advantage of a quick reading of the concentration levels when the 3D camera is at human height, and regardless of its position. We also applied, using a planar UVW Map modifier, a material with a gradient on the diffuse map and a smooth opaque opacity map (Figure 8D). Three heatmaps were carried out to represent distributions for artifacts, individuals under 15 years of age and individuals in secondary positions.

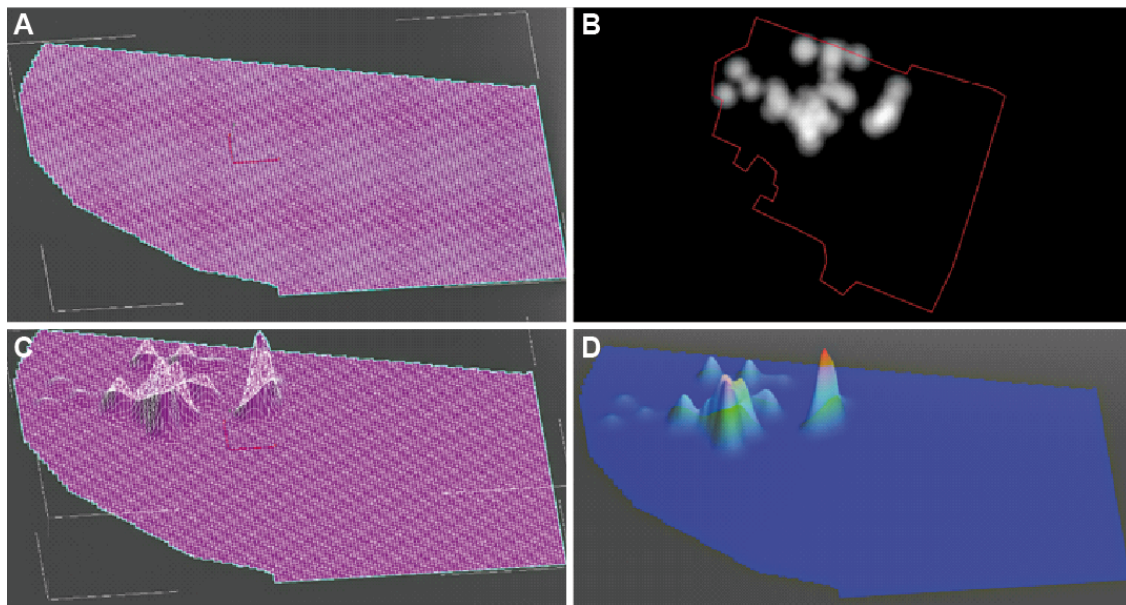


Figure 8. The process of creating a 3D heatmap in 3dsmax. (A) Fine retopologization of the plane intended to undergo the displace modifier; (B) black and white image used for the displace, with contour for recalibration on site; (C) application of the displace modifier; (D) application of a material with a gradient (diffuse map) and an opacity map using a planar UVW map modifier.

3. Results: Towards a Restitution of the Invisible

3.1. The 3D Tool for Landscape Description

The first numerical model of the “bottom of form” terrain allowed a visualization of the site at the time of the archaeological excavation (Figure 9A). It represents the appearance of the substrate after mechanical stripping and the bottom of the sepulchral pits. It is already an interpretive document compared to a snapshot seen from the sky since it allowed one to select the graphic information. Here, only the remains belonging to the occupation phase of the cemetery were selected. The tombs were well delineated topographically to the north of the ditch. Only three pits, resuming somewhat of its orientation, were present immediately to the south. Secondly, and in the absence of preserved superstructures, the restoration of the alto-medieval soil level was only achievable from 3D tools (Figure 9B–D). The position of the tombs, the calculation of their total volume and the stratigraphic reading of their fills makes it possible to propose more or less important stone and soil mounds.

Some liturgical crosses indicating the funerary mounds were added, although no archaeological element allowed us to affirm their presence except for two holes for wedging posts. Their morphology was reconstructed from later illustrations (15th century) [66].

The most popular areas were those where the mounds overlapped the most. The volumes of the mounds appeared more or less identical while their orientations, if the deposits aligned with the underlying excavation, were variable with a west/east dominant. This standardization of grave orientation reflects the will and beliefs of the living [34] where shifts can occur if gravediggers settle on the position of sunrise [67]. In addition to superstructures, empty spaces are identifiable, especially in the center of the area surrounded by mounds with divergent orientations (north/south) compared to the majority of tombs (west/east). An interruption of the edge embankment over a 10 m long section was also clearly visible. It could mark either (i) a chronology of deposits with later burials gradually colonizing the embankment, or (ii) a gateway to the cemetery with a crossing of the ditch, or (iii) a particular burial space, landlocked in the embankment. Finally, the large final volume of the embankment, thrown in its entirety north of the ditch, appeared to be disproportionate to the whole, suggesting that some of the sediments were stored elsewhere. However, despite the care given to the creation of this image, the spatial reading

of the 3D representation of the cemetery can only reflect reality since it is only a fixed image of the landscape without the possibility of taking into account the centuries-old evolution of the site.

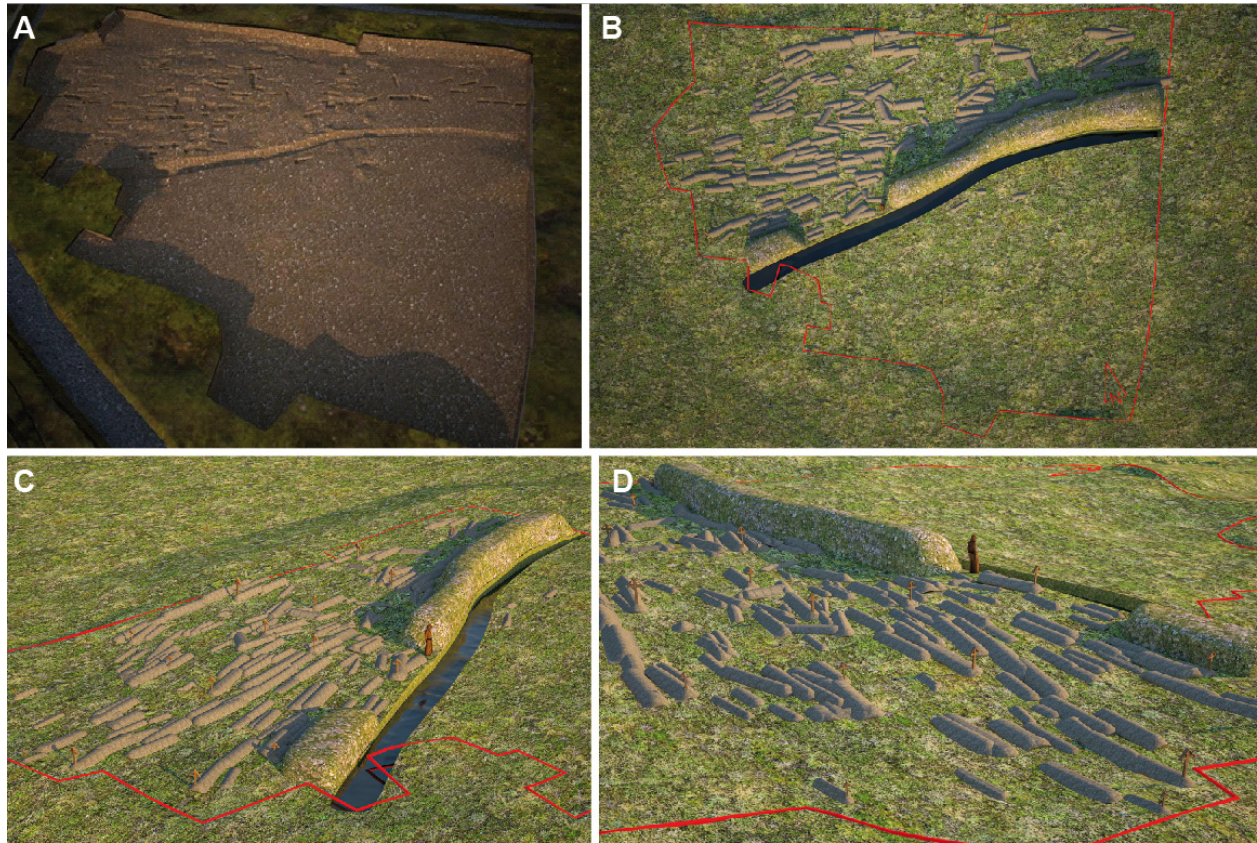


Figure 9. (A) The “bottom of form” DTM. The graves are concentrated north of the border ditch; (B) Zenithal and northwest view of the “funeral mound” DTM graves of different orientations are concentrated north of the bordering ditch; (C,D) View from the west and northwest of the burial mound DTM.

3.2. Subject Distribution (MNI) and Funeral Space Prioritization

The 213 subjects were divided into 140 primary and 73 secondary depots. Nine empty graves bore witness to the post-cemetery layouts. Overall, these changes were numerous, affecting more than one third of the subjects found (73/213 or 34%). The observed secondary deposits were not a true ossuary defined by clusters of bones whose relationship with each subject is forgotten [68]. These deposits were found (i) either in the fills of tombs with subjects in place; (ii) or in ancient tombs according to their shapes and dimensions but where no skeleton in place is preserved; (iii) or finally in archaeological structures not related to funeral events and later. Overall, they concentrated significantly in the northern area of the site, around and in a limestone sarcophagus and at the ditch interruption to a lesser extent (Figure 10A,B). The Moran’s secondary burial index attributed 18.6% of the variance explicable by nearby graves of less than 2 m ($I = 0.186$; $p = 0.0005$), it confirms that these aggregations were therefore neither random nor the result of chance. The establishment of these apparently messy deposits [69] arguably marks the most sought-after locations of the site with a greater breakdown of the premises and more burials in the same place. These places have the most attraction during the time of the site’s occupation. The use of limestone sarcophagi is quite rare on the site as it concerns only six subjects in the primary position (and seven secondary deposits), the bodies being mainly deposited either directly in the pits (34 individuals) or in wooden containers, presumably casings (74 individuals). The presence of sarcophagus can characterize prestigious topographical

situations (i.e., interior of a cult building) that potentially mark spaces dedicated to the memory of the deceased belonging to a specific aristocratic group [70–72]. Their use and reuse by members of the same family have even been demonstrated through DNA [73]. The sarcophagi therefore have an important power of attraction. On the scale of a funeral complex, the spaces are highly codified and possess very different symbolic values from one place to another [28]. In Christian society, the care given to the future of the dead is not limited to that given to the body, the location of the tomb, its depth and its layout are also important social markers [29,30]. Like the theoretical model of central locations [74], the prioritization of spaces probably determines larger services, we were unable to understand the object at this stage of the results, especially for small concentrations observed at the rupture of the border embankment.

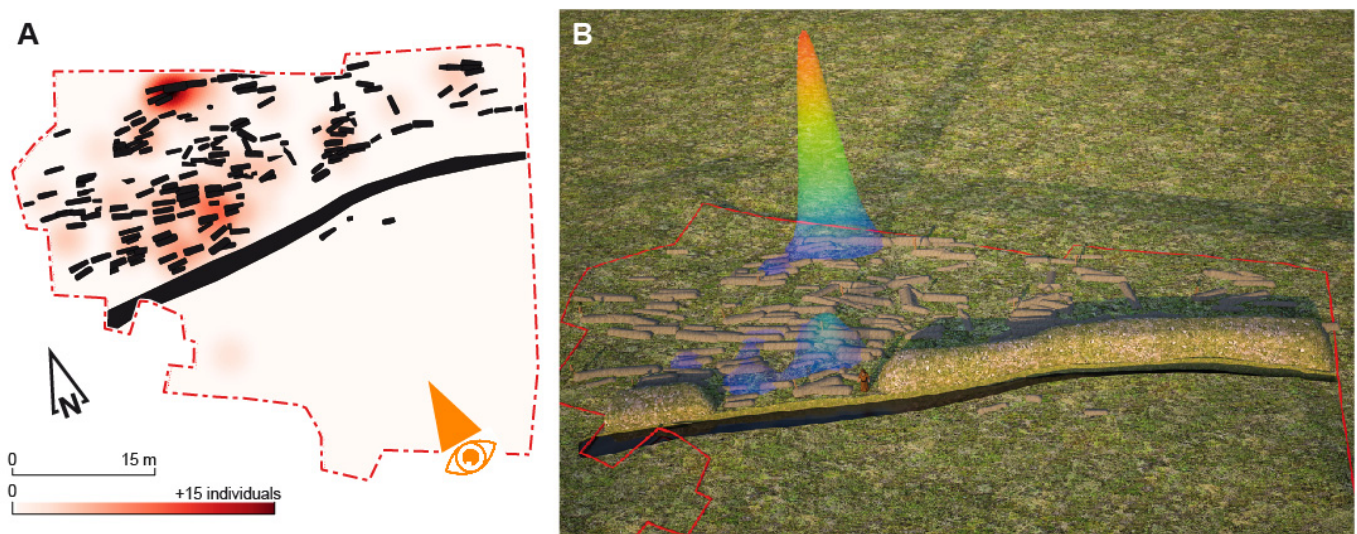


Figure 10. Heatmap representing the concentrations of individuals in secondary positions. Heat map in plan (A) and 3D (B). The eye indicates the direction angle for the 3D restitution.

3.3. Reading the Concentration of Residual Finds

Apart from the secondary deposits, the location of the residual artefacts found in the tombs seemed to us an important element to observe the areas most frequented by the living, where objects are used, broken, forgotten and get lost. These are mostly ceramic shards (27 tombs), fragments of animal bones (6) and a few rare metal objects (8). Of the graves 16% contain them in their fills (35/213 subjects), which produces a background noise representing a diffuse occupation throughout the site. For the most part they are objects in the secondary position, or even residual in the tombs that show more attendance of the living on the graves than real funeral practices. Even the few shroud or clothing pins found come from fills. No burial structure contained all of these materials, but six of them contained two different types. We interpreted the presence of these objects as a witness to the fossilization of a subsynchronous level of circulation linked to domestic or ceremonial activities carried out on the surface in the cemetery, a level dismantled by the excavation of the tombs. The place where these artefacts were found also shows us probably the most used places, the places of passage for the living. Moreover, the distribution of these pits is not coincidental since the Moran's index shows that more than 8% of the variance was explained by concentrations of finds within 3 m, aggregations that were not random ($I = 0.0826$; $p = 0.01533$). Topographically, two large concentrations spaced about ten meters apart (Figure 11A). (i) The most important was near the ditch interruption and about quarantine square meters. It characterized a batch of about ten pits where many subjects are in secondary deposits. (ii) The second center was also located on a dozen graves. These tombs were lined up against a more or less empty space of

tombs of nearly 70 m². This second pole may outline an ancient square in the heart of the cemetery, resulting from the choice to preserve a place from the promiscuity of the graves for non-funeral activities (Figure 11B). Indeed, the historical or archaeological sources of later Christian burial practices clearly show the possible presence of a meeting place, places to preach and pray [28,75]. This coexistence between secular and funeral activities is also well documented in cemeteries in the Middle Ages, where they serve as both a public place, a market and a place of burial [76]. Funeral spaces in the Middle Ages are often considered areas of life and activity, as the historian Philippe Ariès reports, for example, where the ecclesiastical authorities between the 13th and 16th centuries even frequently had to forbid “any person from dancing in the cemetery, from playing any game; forbidden to mimes, jugglers, mask watchers, popular musicians, charlatans to do their suspicious trades there” [77]. Historical sources are less loquacious for the early Middle Ages, but the presence of these soil levels may indicate that these practices are well earlier. Indeed, without historical sources, the statistical 3D reading of the concentration of residual artefacts sheds new light on the organization of the burial space and reinforces the hypothesis of synchronous activities on the surface (circulation?) of the cemetery in some places.

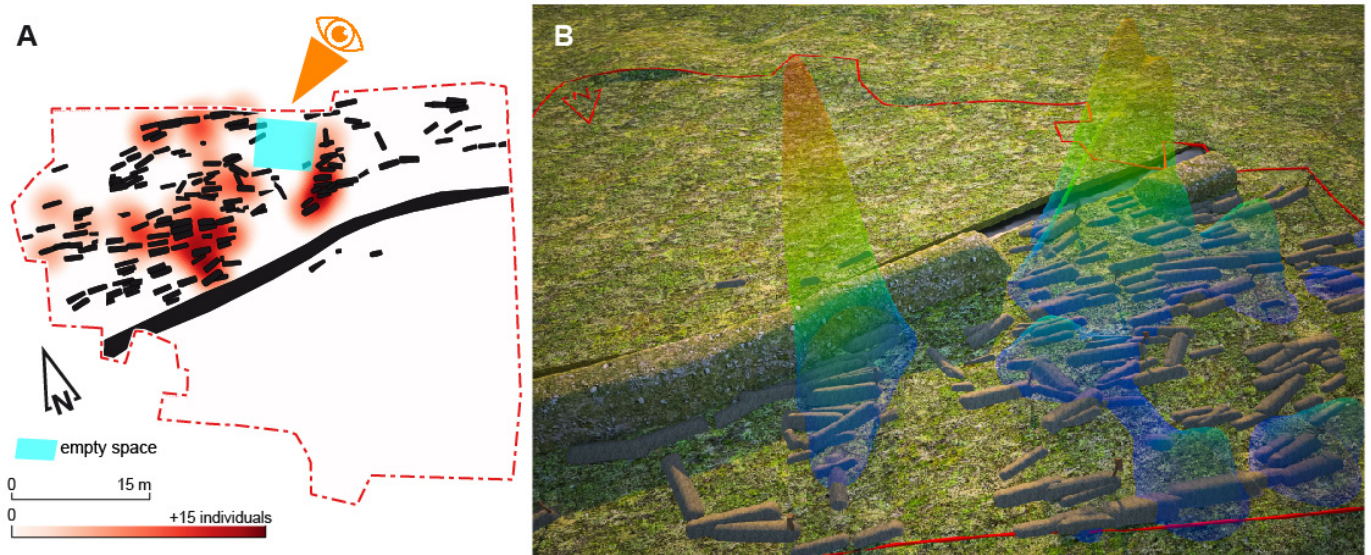


Figure 11. Concentration of all residual artefacts in the tombs. Heat map in plan (A) and 3D (B). The eye indicates the direction angle for the 3D restitution.

3.4. The Organization of the Sepulchral Space by Age at Death

Children under the age of 5 are under-represented in the Olonne-sur-Mer sample, but the rest of the demographic corresponds to a rather natural mortality characteristic of pre-Jennerian parish cemeteries [13,78]. The absence or minimal lack of deficiency of the very young is a recurrent observation in archaeological bone collections [79]. Taphonomic arguments, conservation problems, depth of sepulchral pits or the specialization of spaces according to age at death are often mentioned to explain this phenomenon [9]. Here, the 44 subjects under the age of 15 concentrated significantly in the center of the field, around the empty space already observed previously, spread over several poles. More than 10% of the variance was explained by the search for distant neighbors within 2.5 m (Moran’s $I = 0.1017$; $p = 0.0151$) (Figure 12A,B). These positively correlated self-correlated aggregates suggest a restriction of certain burial spaces by age at death with children who are therefore not systematically buried with their respective families. It is interesting to note that on the periphery of these concentration zones and on the edge of the central empty space, some sepulchral pits had divergent orientations (north/south) compared to the majority

of the population, buried west/east. This observation reinforces the determination of an important attractiveness of the place, since the subjects position graves in defiance of the liturgical rules in force.

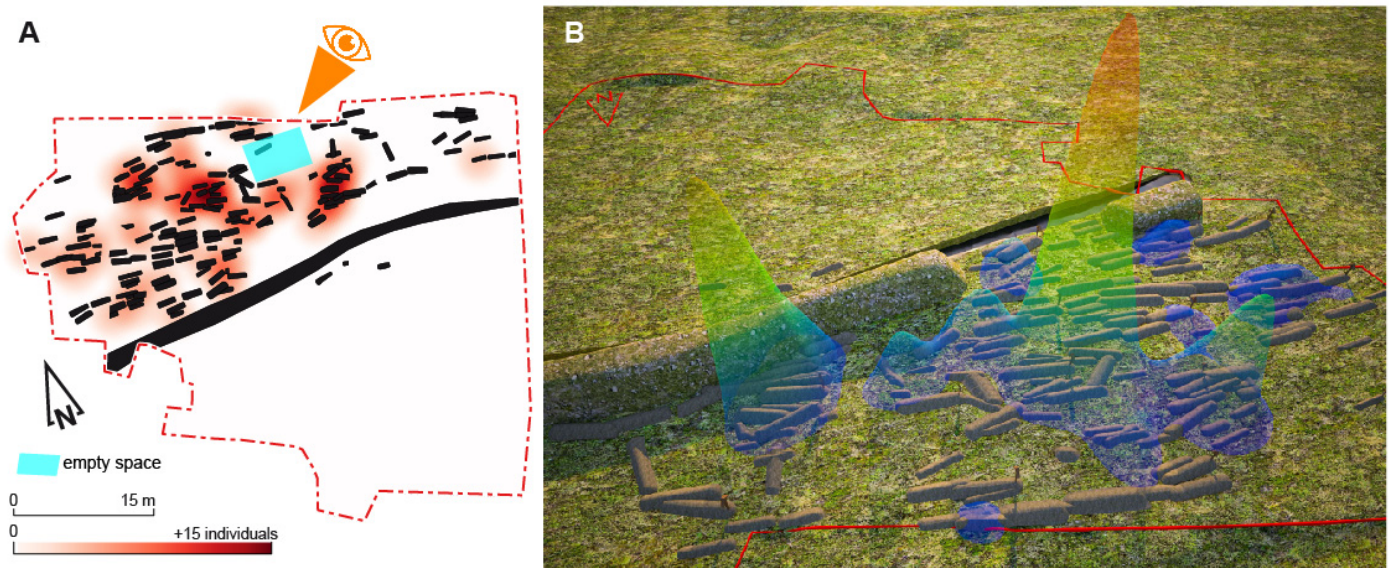


Figure 12. Heatmap for children under the age of 15. Heat map in plan (A) and 3D (B). The eye indicates the direction angle for the 3D restitution.

In similar archaeological contexts, the tombs of the youngest are usually found in privileged places, around churches, under water gutters, *sub stillicidio*, these sites being considered sacred due to the sprinkling of water blessed by the roof [80–83]. In the absence of an identified building foundation, statistical reading of the distribution of children supports the interpretation of the use of this central empty space as genuine liturgical or meeting place for the living. This interpretation also helps to identify more central spaces than others, more favorable for services and offerings.

4. Discussion

The 3D reading coupled with the statistics of the site of Olonne-sur-Mer revealed an interesting archaeological grid, with strengths for the interpretation of spatial data but also weaknesses, especially because of the problems of a dynamic spatial reading. Indeed, the proposed representations accumulate the data recorded over six centuries and did not take into account the evolution of the landscape during the phased period. It is a limitation to keep in mind for the interpretation of spatial elements; possible changes in the vocation of space over time are perfectly possible. This is the case of the interruption observed in the border embankment and the installation of burials closer to the ditch at this location. Perhaps these tombs indicate a chronological underphasing not perceptible at the excavation with a change in the use of this place over time.

Raising the burial mounds and border ditch makes the visualization of a multisecular occupation easy and shows spatial inconsistencies. Although the volume of the embankment appeared disproportionate, it suggests that the soil excavated from the ditch was not entirely thrown up on its edges or that it was regularly maintained with successive digs that were not observed during the excavation. Spots of tombs seemed to sign intentional clusters of subjects, but the anarchical development of superstructures modeled on the variable orientations of the tombs dug into the ground probably did not represent the reality at the extreme end of the use of the cemetery. The burial mounds must have shrunk over time, some graves may have been lost in the collective memory, and the visible part of the tombs must have been more in harmony with each other. The question of the management of

these constrained funerary spaces (because here circumscribed by a ditch) is certainly very important, contrary to open field cemeteries with a less durable use in time and without a defined spatial limit [84–86].

Blank spaces were undoubtedly visible (Figures 11A and 12A), and the statistical analysis allowed us to propose a religious function (i.e., liturgical use as a place to preach) based on the identification of the most sought-after spaces for the dead (secondary and children's burials) and the living (presence of residual furniture). The correlations observed from Moran's index were low (between $I = 0.18$ and 0.08) and explained only a small proportion of the observations. Global and local of spatial autocorrelation analysis have been common in archaeology since the development of GIS, but is currently of limited use in anthropological studies [87–90]. While spatial data are always correlated with each other according to Tobler's First Law of Geography [91–93], the Moran's index represents one of the first developments for reading these correlations [51]. Here, the simplicity of the implementation of this statistical tool, without setting up polygonal geometry, confirms the contribution of this type of approach even if other methods such as HLC (historic landscape characterization) [94,95] or LICD (local indicators for categorical data) could certainly complete and validate the established results [90].

The showcasing of this 3D production to the general public is an aspect that we considered carefully. For this we were considering the use of virtual reality systems for the exploration of this environment, following the example of many other works [96,97]. For some years now, we have had some practice in the use of virtual reality [98,99], but because it belongs to the funerary domain, this type of site is particular and requires a pedagogical support beyond the simple illustration. Before anything else, we think that it is necessary to start an important reflection on what we can or cannot show to a public with heterogeneous sensibilities [100,101].

5. Conclusions

While reality-based 3D surveying and modeling is already widely used in archaeology to calculate precise surfaces, visualize, describe and share information with the public [102,103], their coupling with geostatic tools is still in its early stages in anthropobiology. Beyond the description, this method allows us to go beyond the simple characterization of the data by providing a real interpretation of the management of space by ancient populations. For the Olonne-sur-Mer site, the significant concentrations recorded around an empty space (residual artefacts and younger subjects) are an important argument for a probably liturgical use of this space as a place to preach. The interruption of the edge embankment and the multiple concentrations observed (residual artefacts and secondary deposits) testify to numerous passages and disturbances. These elements also support the interpretation of this space as a place of passage or entrance to the cemetery with a crossing of the ditch, which was not found during the excavation.

Confronting spatial, biological (age at death) and cultural (furniture in secondary position in the tombs) data allows us to test hypotheses of cemetery occupation in an innovative way. Mathematical indices (here Moran's I) allow us to validate this holistic approach for relevant statistical results. The objective of validating or invalidating the hypotheses posed then allows for more detailed work on the archaeological populations, particularly when historical sources are not available [104]. Far from storytelling, these tools allow to support the reasoning by serendipity of archaeologists to reach real conclusions on the evolution of mentalities [27,28].

Author Contributions: Conceptualization, R.C. and J.-B.B.; methodology, R.C. and J.-B.B.; software J.-B.B.; validation, R.C. and J.-B.B.; formal analysis, R.C. and J.-B.B.; investigation, R.C.; resources, R.C.; data curation, R.C.; writing—original draft preparation, R.C. and J.-B.B.; writing—review and editing, R.C. and J.-B.B.; visualization, R.C. and J.-B.B.; supervision, R.C. and J.-B.B.; project administration, R.C.; funding acquisition, R.C. All authors have read and agreed to the published version of the manuscript.

Funding: This research has received funding from the European Union’s Horizon 2020 research and innovation programme under the Marie Skłodowska-Curie grant agreement (No 897565).

Institutional Review Board Statement: Ethical review and approval were waived for archaeological human remains in accordance with French law. The archaeological excavation was the subject of an administrative authorization from the French state on September 14, 2018 (N°2018-714).

Informed Consent Statement: Not applicable.

Data Availability Statement: Human skeletons and all the documentation of the archaeological excavation (primary documentation and excavation report) are preserved by the Regional Archaeological Service of the Pays de la Loire, department of the Vendée, 1 rue Stanislas Baudry BP 63518, 44035 NANTES Cedex 1.

Acknowledgments: This work was supported by the French Regional Archaeology Service of Pays de la Loire (authorization 2018-714), the French National Institute for Preventive Archaeological Research, the UMR 6566 of CNRS and the Marie Skłodowska-Curie individual fellowship, AIDE project for Rozenn Colleter (grant 897565). We are grateful to the reviewers for their commentaries and Philip Miller for editing the English of the manuscript.

Conflicts of Interest: The authors declare no conflict of interest.

Appendix A

Table A1. The 14 Rue de la Paix, Olonne-sur-Mer graves characteristics.

Grave	Length	Width	Depth	Age	Deposit	Funeral Architecture	Area of Decomposition	Volume of the Container/Body	Compacted vol. In Situ	Mound Volume	Type	Block
1	150	36	8	kid	Primary	Coffin	Mixed	0.216	0.21	0.2685	Container	yes
2	220	46	14	adult	Primary	Coffin	Mixed	0.4048	0.45	0.5173	Container	yes
3	200	60	8	adult	Primary	Coffin	Empty	0.48	0.37	0.5725	Container	yes
4	163	64	3	kid	Primary	Coffin	Empty	0.41728	0.2	0.46728	Container	no
5	170	40	18	adult	Primary	Pit	Clogged	0.075	0.21	0.1275	Adult body	yes
6	178	63	3	adult	Primary	Unknown	Unknown	0.075	0.19	0.1225	Adult body	yes
7	80	28	2	kid	Primary	Pit	Mixed	0.037	0.08	0.057	Kid body	no
8	167	42	1	adult	Primary	Unknown	Unknown	0.075	0.17	0.1175	Adult body	no
9	164	45	9	kid	Primary	Unknown	Unknown	0.037	0.18	0.082	Kid body	yes
10	180	70	24	adult	Primary	Coffin	Mixed	0.504	0.22	0.559	Container	yes
11	194	63	24	adult	Primary	Pit	Clogged	0.075	0.38	0.17	Adult body	no
12	195	70	12	adult	Primary	Coffin	Empty	0.546	0.39	0.6435	Container	yes
13	56	35	1	kid	Primary	Unknown	Unknown	0.037	0.08	0.057	Kid body	no
14	160	40	2	adult	Primary	Pit	Clogged	0.075	0.1	0.1	Adult body	no
15	110	40	2	kid	Primary	Pit	Mixed	0.037	0.16	0.077	Kid body	no
16	175	62	12	adult	Primary	Coffin	Mixed	0.434	0.37	0.5265	Container	yes
17	176	60	2	adult	Primary	Unknown	Unknown	0.075	0.18	0.12	Adult body	yes
18	180	80	30	kid	Primary	Coffin	Empty	0.576	0.61	0.7285	Container	yes
19	210	60	2	adult	Primary	Coffin	Empty	0.504	0.29	0.5765	Container	yes
20	200	58	16	adult	Primary	Pit	Clogged	0.075	0.23	0.1325	Adult body	yes
21	164	50	2	none	Empty	Unknown	Empty	0.328	0.24	0.388	Container	no
22	34	55	14	kid	Primary	Unknown	Unknown	0.037	0.16	0.077	Kid body	no
23	170	73	21	adult	Primary	Coffin	Empty	0.4964	0.16	0.5364	Container	no
24	100	45	1	adult	Primary	Unknown	Unknown	0.075	0.09	0.0975	Adult body	no
25	70	50	2	adult	Secondary	Pit	Clogged	0.075	0.05	0.0875	Adult body	no
26	220	52	14	adult	Primary	Coffin	Empty	0.4576	0.29	0.5301	Container	no
27	40	40	3	kid	Primary	Unknown	Unknown	0.037	0.08	0.057	Kid body	no
28	190	60	4	adult	Primary	Pit	Clogged	0.075	0.25	0.1375	Adult body	yes
29	160	55	10	adult	Primary	Coffin	Empty	0.352	0.23	0.4095	Container	yes

Table A1. Cont.

Grave	Length	Width	Depth	Age	Deposit	Funeral Architecture	Area of Decomposition	Volume of the Container/Body	Compacted vol. In Situ	Mound Volume	Type	Block
30	250	55	30	adult	Primary	Pit	Mixed	0.075	0.29	0.1475	Adult body	yes
31	200	75	26	adult	Primary	Coffin	Empty	0.6	0.59	0.7475	Container	yes
32	60	50	2	adult	Secondary	Unknown	Unknown	0.075	0.05	0.0875	Adult body	yes
33	170	55	8	adult	Primary	Coffin	Empty	0.374	0.24	0.434	Container	yes
34	180	63	24	adult	Primary	Pit	Clogged	0.075	0.4	0.175	Adult body	yes
35	100	45	2	kid	Primary	Coffin	Mixed	0.18	0.08	0.2	Container	yes
36	210	80	24	adult	Secondary	Sarcophagus	Empty	0.672	0.53	0.8045	Container	yes
37	223	65	5	adult	Primary	Pit	Mixed	0.075	0.4	0.175	Adult body	no
38	154	40	5	kid	Primary	Coffin	Empty	0.2464	0.07	0.2639	Container	no
39	190	55	5	adult	Primary	Unknown	Unknown	0.075	0.19	0.1225	Adult body	yes
40	184	56	10	adult	Primary	Sarcophagus	Clogged	0.41216	0.31	0.48966	Container	yes
41	188	50	40	adult	Primary	Pit	Clogged	0.075	0.42	0.18	Adult body	yes
42	178	56	12	adult	Primary	Pit	Clogged	0.075	0.2	0.125	Adult body	yes
43	130	40	1	adult	Primary	Pit	Clogged	0.075	0.11	0.1025	Adult body	no
44	130	44	1	adult	Primary	Unknown	Clogged	0.075	0.07	0.0925	Adult body	no
45	216	61	25	adult	Primary	Coffin	Empty	0.52704	0.5	0.65204	Container	no
47	195	65	17	adult	Primary	Coffin	Empty	0.507	0.39	0.6045	Container	yes
48	185	65	9	adult	Primary	Pit	Clogged	0.075	0.13	0.1075	Adult body	no
49	126	56	24	kid	Primary	Coffin	Empty	0.28224	0.29	0.35474	Container	yes
50	180	60	1	adult	Secondary	Unknown	Unknown	0.075	0.1	0.1	Adult body	yes
51	200	70	5	adult	Secondary	Sarcophagus	Empty	0.56	0.23	0.6175	Container	no
52	193	60	15	adult	Primary	Coffin	Empty	0.4632	0.3	0.5382	Container	yes
53	100	36	5	kid	Primary	Pit	Clogged	0.037	0.21	0.0895	Kid body	yes
54	72	30	3	kid	Primary	Unknown	Unknown	0.037	0.07	0.0545	Kid body	no
55	206	60	15	adult	Primary	Coffin	Clogged	0.075	0.47	0.1925	Adult body	yes
56	48	37	7	kid	Primary	Unknown	Unknown	0.037	0.05	0.0495	Kid body	no
57	80	60	5	adult	Primary	Unknown	Unknown	0.075	0.09	0.0975	Adult body	no
58	200	60	2	adult	Secondary	Sarcophagus	Empty	0.48	0.35	0.5675	Container	yes
59	185	70	10	adult	Primary	Coffin	Clogged	0.075	0.42	0.18	Adult body	yes
60	185	63	7	adult	Primary	Coffin	Empty	0.4662	0.23	0.5237	Container	no
61	143	50	10	kid	Primary	Coffin	Empty	0.286	0.17	0.3285	Container	no
62	190	62	5	adult	Secondary	Unknown	Unknown	0.075	0.57	0.2175	Adult body	yes
63	175	66	7	adult	Secondary	Unknown	Unknown	0.075	0.54	0.21	Adult body	no
64	133	48	8	kid	Primary	Coffin	Clogged	0.037	0.11	0.0645	Kid body	yes
65	168	50	5	adult	Primary	Pit	Clogged	0.075	0.14	0.11	Adult body	yes
66	260	50	3	adult	Primary	Coffin	Empty	0.52	0.25	0.5825	Container	yes
67	200	63	4	adult	Secondary	Unknown	Unknown	0.075	0.34	0.16	Adult body	yes
68	190	50	20	adult	Primary	Coffin	Empty	0.38	0.29	0.4525	Container	yes
69	163	50	12	adult	Primary	Coffin	Mixed	0.326	0.32	0.406	Container	yes
70	186	68	4	adult	Primary	Pit	Empty	0.50592	0.37	0.59842	Container	no
71	60	45	6	adult	Primary	Unknown	Clogged	0.075	0.04	0.085	Adult body	no
72	190	50	13	adult	Primary	Pit	Mixed	0.075	0.27	0.1425	Adult body	no
73	120	60	12	kid	Primary	Coffin	Empty	0.288	0.23	0.3455	Container	yes
74	30	60	12	none	Empty	Unknown	Empty	0.072	0.03	0.0795	Container	yes
75	200	55	40	kid	Primary	Coffin	Empty	0.44	0.59	0.5875	Container	yes
76	140	48	10	kid	Primary	Coffin	Empty	0.2688	0.2	0.3188	Container	yes
77	210	56	12	adult	Primary	Coffin	Empty	0.4704	0.29	0.5429	Container	no
78	174	60	3	adult	Primary	Pit	Clogged	0.075	0.19	0.1225	Adult body	yes
79	195	64	3	adult	Secondary	Unknown	Unknown	0.075	0.16	0.115	Adult body	yes
80	197	68	35	adult	Primary	Coffin	Clogged	0.075	0.5	0.2	Adult body	yes
81	200	75	3	adult	Secondary	Unknown	Unknown	0.075	0.33	0.1575	Adult body	yes
82	200	60	3	adult	Secondary	Unknown	Unknown	0.075	0.28	0.145	Adult body	yes

Table A1. Cont.

Grave	Length	Width	Depth	Age	Deposit	Funeral Architecture	Area of Decomposition	Volume of the Container/Body	Compacted vol. In Situ	Mound Volume	Type	Block
83	120	45	11	kid	Primary	Unknown	Clogged	0.037	0.15	0.0745	Kid body	yes
84	115	50	1	kid	Primary	Coffin	Empty	0.23	0.06	0.245	Container	yes
85	205	66	13	adult	Secondary	Unknown	Unknown	0.075	0.34	0.16	Adult body	yes
86	260	62	8	adult	Secondary	Unknown	Unknown	0.075	0.34	0.16	Adult body	no
87	208	70	22	adult	Secondary	Unknown	Unknown	0.075	0.6	0.225	Adult body	yes
88	140	44	23	kid	Primary	Pit	Clogged	0.037	0.26	0.102	Kid body	yes
89	110	45	3	adult	Primary	Unknown	Empty	0.198	0.07	0.2155	Container	yes
90	146	42	8	kid	Primary	Coffin	Empty	0.24528	0.14	0.28028	Container	yes
91	240	77	26	adult	Primary	Pit	Empty	0.7392	0.65	0.9017	Container	no
92	180	60	1	adult	Primary	Unknown	Unknown	0.075	0.16	0.115	Adult body	yes
93	136	60	17	adult	Primary	Coffin	Empty	0.3264	0.25	0.3889	Container	yes
94	75	50	2	adult	Primary	Pit	Clogged	0.075	0.1	0.1	Adult body	yes
95	200	75	18	adult	Primary	Coffin	Empty	0.6	0.44	0.71	Container	yes
96	200	72	30	adult	Primary	Coffin	Empty	0.576	0.58	0.721	Container	yes
97	170	60	44	adult	Secondary	Unknown	Unknown	0.075	0.63	0.2325	Adult body	yes
98	245	80	16	adult	Primary	Sarcophagus	Empty	0.784	0.41	0.8865	Container	yes
99	158	60	5	none	Empty	Unknown	Empty	0.3792	0.16	0.4192	Container	yes
100	120	38	5	kid	Secondary	Unknown	Unknown	0.037	0.09	0.0595	Kid body	yes
101	106	45	12	none	Empty	Unknown	Empty	0.1908	0.09	0.2133	Container	yes
102	195	70	2	adult	Primary	Coffin	Empty	0.546	0.24	0.606	Container	yes
103	123	30	10	kid	Primary	Pit	Clogged	0.037	0.09	0.0595	Kid body	no
104	190	70	2	adult	Primary	Unknown	Unknown	0.075	0.21	0.1275	Adult body	no
106	193	60	20	adult	Primary	Coffin	Empty	0.4632	0.21	0.5157	Container	yes
107	205	44	10	adult	Primary	Coffin	Empty	0.3608	0.13	0.3933	Container	yes
108	198	48	11	adult	Primary	Coffin	Empty	0.38016	0.23	0.43766	Container	yes
109	196	63	5	none	Empty	Unknown	Empty	0.49392	0.32	0.57392	Container	yes
110	50	34	9	kid	Primary	Coffin	Empty	0.068	0.04	0.078	Container	yes
111	230	80	10	adult	Secondary	Unknown	Unknown	0.075	0.27	0.1425	Adult body	no
112	250	54	20	adult	Primary	Unknown	Unknown	0.075	0.49	0.1975	Adult body	yes
113	200	54	2	none	Empty	Unknown	Empty	0.432	0.34	0.517	Container	yes
114	220	63	2	adult	Primary	Coffin	Empty	0.5544	0.2	0.6044	Container	no
115	110	32	7	kid	Primary	Pit	Clogged	0.037	0.1	0.062	Kid body	yes
116	210	78	16	adult	Primary	Coffin	Empty	0.6552	0.4	0.7552	Container	yes
117	180	50	24	adult	Primary	Coffin	Empty	0.36	0.17	0.4025	Container	yes
118	236	50	5	adult	Secondary	Unknown	Unknown	0.075	0.23	0.1325	Adult body	no
119	187	62	15	adult	Primary	Coffin	Empty	0.46376	0.18	0.50876	Container	yes
120	186	75	10	adult	Primary	Unknown	Unknown	0.075	0.11	0.1025	Adult body	yes
121	65	62	20	adult	Primary	Coffin	Empty	0.1612	0.03	0.1687	Container	yes
122	199	54	11	adult	Primary	Coffin	Empty	0.42984	0.27	0.49734	Container	yes
123	130	60	8	adult	Primary	Coffin	Empty	0.312	0.18	0.357	Container	no
124	151	43	2	adult	Primary	Unknown	Empty	0.25972	0.1	0.28472	Container	yes
125	195	60	30	adult	Primary	Coffin	Empty	0.468	0.36	0.558	Container	yes
126	80	40	10	adult	Primary	Pit	Clogged	0.075	0.08	0.095	Adult body	yes
127	120	50	7	kid	Primary	Unknown	Mixed	0.037	0.15	0.0745	Kid body	yes
128	140	68	8	kid	Primary	Unknown	Unknown	0.037	0.12	0.067	Kid body	yes
129	70	70	10	adult	Primary	Unknown	Unknown	0.075	0.08	0.095	Adult body	yes
130	220	55	2	adult	Primary	Unknown	Unknown	0.075	0.02	0.08	Adult body	yes
131	210	55	28	adult	Primary	Pit	Empty	0.462	0.53	0.5945	Container	yes
132	180	80	2	adult	Primary	Pit	Clogged	0.075	0.22	0.13	Adult body	yes
133	70	40	10	kid	Primary	Unknown	Unknown	0.037	0.05	0.0495	Kid body	no
134	180	50	7	adult	Secondary	Unknown	Empty	0.36	0.23	0.4175	Container	yes
135	196	60	2	adult	Primary	Unknown	Empty	0.4704	0.26	0.5354	Container	yes
136	180	70	10	none	Empty	Unknown	Empty	0.504	0.28	0.574	Container	no
137	140	44	28	kid	Primary	Coffin	Empty	0.2464	0.11	0.2739	Container	yes
138	200	50	5	kid	Primary	Unknown	Unknown	0.037	0.24	0.097	Kid body	yes
139	211	50	17	adult	Primary	Coffin	Empty	0.422	0.33	0.5045	Container	yes
140	230	60	30	adult	Primary	Coffin	Empty	0.552	0.37	0.6445	Container	yes

Table A1. Cont.

Grave	Length	Width	Depth	Age	Deposit	Funeral Architecture	Area of Decomposition	Volume of the Container/Body	Compacted vol. In Situ	Mound Volume	Type	Block
141	230	66	20	adult	Primary	Pit	Clogged	0.075	0.29	0.1475	Adult body	yes
142	190	44	16	adult	Primary	Coffin	Empty	0.3344	0.33	0.4169	Container	yes
143	215	55	16	adult	Primary	Coffin	Empty	0.473	0.34	0.558	Container	yes
144	90	40	5	adult	Primary	Coffin	Empty	0.144	0.2	0.194	Container	yes
145	185	40	10	adult	Primary	Coffin	Empty	0.296	0.16	0.336	Container	yes
146	70	50	2	adult	Primary	Unknown	Empty	0.14	0.22	0.195	Container	no
147	150	77	10	adult	Secondary	Unknown	Unknown	0.075	0.32	0.155	Adult body	yes
148	140	38	2	none	Empty	Unknown	Empty	0.2128	0.18	0.2578	Container	yes
149	180	56	20	adult	Primary	Coffin	Empty	0.4032	0.31	0.4807	Container	yes
150	120	57	20	adult	Primary	Coffin	Empty	0.2736	0.19	0.3211	Container	yes
151	210	73	25	adult	Primary	Coffin	Empty	0.6132	0.53	0.7457	Container	yes
152	188	55	16	adult	Primary	Coffin	Empty	0.4136	0.31	0.4911	Container	yes
153	185	50	14	adult	Primary	Coffin	Empty	0.37	0.17	0.4125	Container	yes
154	180	40	60	adult	Primary	Unknown	Unknown	0.075	0.12	0.105	Adult body	no
155	160	54	8	adult	Primary	Coffin	Empty	0.3456	0.21	0.3981	Container	yes
156	150	75	25	kid	Primary	Unknown	Unknown	0.037	0.22	0.092	Kid body	yes
157	220	58	17	adult	Primary	Pit	Clogged	0.075	0.24	0.135	Adult body	yes
158	220	65	7	adult	Primary	Coffin	Empty	0.572	0.49	0.6945	Container	yes
159	173	70	30	kid	Primary	Unknown	Unknown	0.037	0.25	0.0995	Kid body	yes
160	220	71	16	adult	Primary	Coffin	Empty	0.6248	0.57	0.7673	Container	yes
161	180	60	30	adult	Primary	Coffin	Empty	0.432	0.18	0.477	Container	yes
162	150	46	24	kid	Primary	Coffin	Empty	0.276	0.22	0.331	Container	yes
163	180	45	8	adult	Primary	Pit	Clogged	0.075	0.27	0.1425	Adult body	no
164	165	63	5	kid	Primary	Unknown	Unknown	0.037	0.3	0.112	Kid body	yes
165	220	55	25	adult	Primary	Pit	Clogged	0.075	0.53	0.2075	Adult body	yes
166	230	80	30	adult	Secondary	Unknown	Unknown	0.075	0.95	0.3125	Adult body	yes
167	210	80	10	adult	Secondary	Sarcophagus	Empty	0.672	0.3	0.747	Container	yes
168	80	60	10	adult	Primary	Pit	Clogged	0.075	0.06	0.09	Adult body	yes
169	175	60	25	adult	Primary	Coffin	Empty	0.42	0.2	0.47	Container	yes
170	120	40	18	kid	Primary	Coffin	Empty	0.192	0.13	0.2245	Container	yes
171	180	50	20	adult	Primary	Pit	Clogged	0.075	0.25	0.1375	Adult body	yes
172	90	55	6	adult	Primary	Unknown	Unknown	0.075	0.21	0.1275	Adult body	yes
173	140	45	20	kid	Primary	Coffin	Empty	0.252	0.2	0.302	Container	yes
174	220	65		none	Empty	Unknown	Empty	0.572	0.3	0.647	Container	no

References

- Meyer-Heß, M.F. Identification of Archaeologically Relevant Areas Using Open Geodata. *KN J. Cartogr. Geogr. Inf.* **2020**, *70*, 107–125. [\[CrossRef\]](#)
- Canuto, M.A.; Estrada-Belli, F.; Garrison, T.G.; Houston, S.D.; Acuña, M.J.; Kováč, M.; Marken, D.; Nondédéo, P.; Auld-Thomas, L.; Castanet, C.; et al. Ancient lowland Maya complexity as revealed by airborne laser scanning of northern Guatemala. *Science* **2018**, *361*, eaau0137. [\[CrossRef\]](#)
- Inomata, T.; Pinzón, F.; Ranchos, J.L.; Haraguchi, T.; Nasu, H.; Fernandez-Diaz, J.C.; Aoyama, K.; Yonenobu, H. Archaeological Application of Airborne LiDAR with Object-Based Vegetation Classification and Visualization Techniques at the Lowland Maya Site of Ceibal, Guatemala. *Remote Sens.* **2017**, *9*, 563. [\[CrossRef\]](#)
- Chase, A.F.; Chase, D.Z.; Weishampel, J.F.; Drake, J.B.; Shrestha, R.L.; Slatton, K.C.; Awe, J.J.; Carter, W.E. Airborne LiDAR, archaeology, and the ancient Maya landscape at Caracol, Belize. *J. Archaeol. Sci.* **2011**, *38*, 387–398. [\[CrossRef\]](#)
- Wang, S.; Hu, Q.; Wang, F.; Ai, M.; Zhong, R. A Microtopographic Feature Analysis-Based LiDAR Data Processing Approach for the Identification of Chu Tombs. *Remote Sens.* **2017**, *9*, 880. [\[CrossRef\]](#)
- Evers, R.; Masters, P. The application of low-altitude near-infrared aerial photography for detecting clandestine burials using a UAV and low-cost unmodified digital camera. *Forensic Sci. Int.* **2018**, *289*, 408–418. [\[CrossRef\]](#)
- Poirier, N.; Hautefeuille, F.; Calastrenc, C. Low Altitude Thermal Survey by Means of an Automated Unmanned Aerial Vehicle for the Detection of Archaeological Buried Structures. *Archaeol. Prospect.* **2013**, *20*, 303–307. [\[CrossRef\]](#)
- Cochet, A. *La Normandie Souterraine Ou Notice Sur des Cimetières Romains et Des Cimetières Francs Explorés En Normandie*; Derache: Paris, France, 1855.
- Bonnabel, L. *Archéologie de La Mort En France; La Découverte*: Paris, France, 2012.

10. Bowman, S. Interpreting the Past. In *Radiocarbon Dating*; University of California Press: Berkeley, CA, USA, 1990; ISBN 978-0-520-07037-0.
11. Schoeninger, M.J.; Moore, K. Bone stable isotope studies in archaeology. *J. World Prehistory* **1992**, *6*, 247–296. [[CrossRef](#)]
12. Handt, O.; Höss, M.; Krings, M.; Pääbo, S. Ancient DNA: Methodological challenges. *Cell. Mol. Life Sci.* **1994**, *50*, 524–529. [[CrossRef](#)] [[PubMed](#)]
13. Hoppa, R.D.; Vaupel, J.W. *Paleodemography: Age Distributions from Skeletal Samples*; Cambridge University Press: Cambridge, UK, 2008; ISBN 978-1-139-44155-1.
14. Colleter, R.; Bataille, C.P.; Dabernat, H.; Pichot, D.; Hamon, P.; Duchesne, S.; Labaune-Jean, F.; Jean, S.; Le Cloirec, G.; Milano, S.; et al. The Last Battle of Anne of Brittany: Solving Mass Grave through an Interdisciplinary Approach (Paleopathology, Biological anthropology, History, Multiple Isotopes and Radiocarbon Dating). *bioRxiv* **2021**. [[CrossRef](#)]
15. Duday, H.; Cipriani, A.; Pearce, J. *The Archaeology of the Dead: Lectures in Archaeoanthatology*; Oxbow Books: Oxford, UK; Oakville, ON, Canada, 2009. [[CrossRef](#)]
16. Metcalf, P.; Huntington, R. *Celebrations of Death: The Anthropology of Mortuary Ritual*; Cambridge University Press: Cambridge, UK, 1995; ISBN 978-0-521-42375-5.
17. Haglund, W.D.; Sorg, M.H. *Advances in Forensic Taphonomy: Method, Theory, and Archaeological Perspectives*; CRC Press: Boca Raton, FL, USA, 2001; ISBN 978-1-4200-5835-2.
18. Duday, H. Archaeoanthatology or the Archaeology of Death. In *The Social Archaeology of Funerary Remains*; Oxbow Books: Oxford, UK, 2009; pp. 30–56. ISBN 978-1-78297-270-9.
19. Kazanski, M.; Périn, P.; Vallet, F. *L'Or des Princes Barbares: Du Caucase à la Gaule, Ve siècle après J.-C.: [expositions] Musée des antiquités nationales, Château de Saint-Germain-en-Laye, 26 septembre 2000-8 janvier 2001, Reiss-Museum Mannheim, 11 février-4 juin 2001*; Éditions de la Réunion des Musées Nationaux: Paris, France, 2000; ISBN 978-2-7118-3660-4.
20. Holliday, V.T.; Gartner, W.G. Methods of soil P analysis in archaeology. *J. Archaeol. Sci.* **2007**, *34*, 301–333. [[CrossRef](#)]
21. Cowley, D. Remote Sensing for Archaeological Heritage Management. In Proceedings of the 11th EAC Heritage Management Symposium, Reykjavík, Iceland, 25–27 March 2010; Europae Archaeologia Consilium: Brussel, Belgium, 2011; Volume 5, ISBN 978-963-9911-20-8.
22. Bayliss, A. *Anglo-Saxon Graves and Grave Goods of the 6th and 7th Centuries AD: A Chronological Framework*; Routledge: London, UK, 2017; ISBN 978-1-351-57646-8.
23. Steckel, R.H. What Can Be Learned from Skeletons that Might Interest Economists, Historians, and Other Social Scientists? *Am. Econ. Rev.* **2003**, *93*, 213–220. [[CrossRef](#)]
24. Allentoft, M.E.; Sikora, M.; Sjögren, K.-G.; Rasmussen, S.; Rasmussen, M.; Stenderup, J.; Damgaard, P.D.B.; Schroeder, H.; Ahlström, T.; Vinner, L.; et al. Population genomics of Bronze Age Eurasia. *Nat. Cell Biol.* **2015**, *522*, 167–172. [[CrossRef](#)] [[PubMed](#)]
25. Margaryan, A.; Lawson, D.J.; Sikora, M.; Racimo, F.; Rasmussen, S.; Moltke, I.; Cassidy, L.M.; Jørsboe, E.; Ingason, A.; Pedersen, M.W.; et al. Population genomics of the Viking world. *Nat. Cell Biol.* **2020**, *585*, 390–396. [[CrossRef](#)]
26. Testart, A. *Les Morts d'accompagnement. La Servitude Volontaire I*; Errance: Paris, France, 2004.
27. Crubézy, É.; Nikolaeva, D. *Vainqueurs Ou Vaincus? L'énigme de La Iakoutie*; Odile Jacob: Paris, France, 2017; ISBN 978-2-7381-3791-3.
28. Colleter, R. *Pratiques Funéraires, Squelettes et Inégalités Sociales. Étude d'un Echantillon des Elites Bretonnes à l'Époque Moderne*. Ph.D. Thesis, Université Paul Sabatier Toulouse III, Toulouse, France, 2018.
29. Croix, A. *La Bretagne Aux XVIe et XVIIe Siècles. La vie, La Mort, La Foi*; Maloine: Paris, France, 1981.
30. Vovelle, M. La Mort et l'Occident. De 1300 à Nos Jours. In *Bibliothèque des Histoires, Série illustrée*; Gallimard: Paris, France, 2000.
31. Pearson, M.P. *The Archaeology of Death and Burial*; Sutton Publishing Ltd.: Gloucestershire, UK, 1999; ISBN 978-0-7509-1777-3.
32. Colleter, R.; Chauveau, C.; Coffineau, E.; Cotté, O.; Deloze, V.; Hinguant, S.; Labaune-Jean, F.; Leboucher, F.; Peytremann, E. *Du Cimetière du Haut Moyen Âge au Bourg Prioral: Olonne-sur-Mer (85), 14 Rue de la Paix. Volume 1, Texte et Inventaire*; Inrap Grand-Ouest: Cesson-Sévigné, France, 2020; p. 337.
33. Noterman, A.; Cervel, M. *Ritualiser, Gérer, Piller. Rencontre Autour des Réouvertures de Tombes et de La Manipulation Des Ossements. Actes de La 9e Rencontre Du Gaaf, 10–12 Mai 2017, Poitiers*; Publications du Gaaf: Poitiers, France, 2020.
34. Lorans, E. Le monde des morts de l'Antiquité tardive à l'époque moderne (IVe-XIXe s.). In *Archéologie Funéraire*; Ferdière, A., Ed.; Éditions Errance: Paris, France, 2000; pp. 155–197.
35. Crubézy, É.; Duday, H.; Sellier, P.; Tillier, A.-M. Anthropologie et Archéologie: Dialogue Sur Les Ensembles Funéraires. *Bull. Mémoires Société Anthropologie Paris* **1990**, *2*, 5–12.
36. Duday, H. L'archéoanthatologie ou l'archéologie de la mort. In *Objets et Méthodes en Paléoanthropologie*; Comité des Travaux Historiques et Scientifique: Paris, France, 2005; pp. 153–207.
37. Colleter, R.; Romain, J.-B.; Barreau, J.-B. HumanOS: An open source nomadic software database for physical anthropology and archaeology. *Virtual Archaeol. Rev.* **2020**, *11*, 94–105. [[CrossRef](#)]
38. Duday, H.; Courtaud, P.; Crubezy, É.; Sellier, P.; Tillier, A.-M. L'Anthropologie «de terrain»: Reconnaissance et interprétation des gestes funéraires. *Bull. Mém. Soc. d'Anthropol. Paris* **1990**, *2*, 29–49. [[CrossRef](#)]
39. Schmitt, A. Une nouvelle méthode pour estimer l'âge au décès des adultes à partir de la surface sacro-pelvienne iliaque. *Bull. Mém. Soc. Anthropol. Paris* **2005**, *17*, 89–101.
40. Lovejoy, C.O. Dental wear in the Libben population: Its functional pattern and role in the determination of adult skeletal age at death. *Am. J. Phys. Anthr.* **1985**, *68*, 47–56. [[CrossRef](#)] [[PubMed](#)]

41. Lovejoy, C.O.; Meindl, R.S.; Mensforth, R.P.; Barton, T.J. Multifactorial determination of skeletal age at death: A method and blind tests of its accuracy. *Am. J. Phys. Anthr.* **1985**, *68*, 1–14. [[CrossRef](#)] [[PubMed](#)]
42. Moorrees, C.F.; Fanning, E.A.; Hunt, E.E. Age Variation of Formation Stages for Ten Permanent Teeth. *J. Dent. Res.* **1963**, *42*, 1490–1502. [[CrossRef](#)]
43. Moorrees, C.F.A.; Fanning, E.A.; Hunt, E.E. Formation and resorption of three deciduous teeth in children. *Am. J. Phys. Anthr.* **1963**, *21*, 205–213. [[CrossRef](#)]
44. Stloukal, M.; Hanáková, M. Die Längeder Langsknocher Altawisher Bevölkerungen Unter Besonderer Berücksichtigung von Wachstum Fragen. *Homo* **1978**, *29*, 53–59.
45. Birkner, R. *L'image Radiologique Typique du Squelette: Aspect Normal et Variantes chez l'Adulte et l'Enfant; pour Médecins, Etudiants et Manipulateurs*; Maloine: Paris, France, 1980; ISBN 2-224-00568-7.
46. Owings Webb, P.A.; Myers Suchey, J. Epiphyseal Union of the Anterior Iliac Crest and Medial Clavicle in a Modern Multiracial Sample of American Males and Females. *Am. J. Phys. Anthropol.* **1985**, *68*, 457–466. [[CrossRef](#)]
47. Sellier, P. L'estimation de l'âge des foetus et des enfants morts en période périnatale: Une révision de Fazekas et Kosa (1978). In Proceedings of the Croissance et Vieillesse, Actes du 21^{ème} Colloque du Groupement des Anthropologistes de Langue Française, Bordeaux, France, 13–15 May 1993.
48. Sellier, P.; Tillier, A.-M.; Bruzek, J. A la recherche d'une référence pour l'estimation de l'âge des foetus, nouveau-nés et nour-rissons des populations archéologiques européennes. *Anthropol. Préhistoire* **1997**, *108*, 75–87.
49. Scheuer, L.; Black, S.M. *Developmental Juvenile Osteology*; Academic Press: San Diego, CA, USA, 2000; ISBN 0-12-624000-0.
50. Oliveau, S. Autocorrélation spatiale: Leçons du changement d'échelle. *L'Espace Géographique* **2010**, *39*, 51–64. [[CrossRef](#)]
51. Moran, P.A.P. The Interpretation of Statistical Maps. *J. R. Stat. Soc. Ser. B* **1948**, *10*, 243–251. [[CrossRef](#)]
52. Guisan, A.; Thuiller, W.; Zimmermann, N.E. *Habitat Suitability and Distribution Models with Applications in R*; Cambridge University Press: Cambridge, UK, 2017.
53. Sillero, N.; Gomes, V. Living in clusters: The local spatial segregation of a lizard community. *Basic Appl. Herpetol.* **2016**, *30*, 61–75. [[CrossRef](#)]
54. Simon, F.J.V. DEMto3D, Impresión 3D de Modelos Del Terreno. Available online: <https://demto3d.com/> (accessed on 8 February 2021).
55. Halstead, M.; Kass, M.; Derose, T. Efficient, fair interpolation using Catmull-Clark surfaces. In Proceedings of the 20th annual conference on Computer graphics and interactive techniques—SIGGRAPH '93, Anaheim, CA, USA, 9–13 August 1993; pp. 35–44.
56. Baojun, W.; Bin, S.; Zhen, S. A simple approach to 3D geological modelling and visualization. *Bull. Int. Assoc. Eng. Geol.* **2009**, *68*, 559–565. [[CrossRef](#)]
57. Diana, A. Edge Chamfering Algorithm. Master's Thesis, Institute of Computer Science Computer Science Curriculum, University of Tartu, Tartu, Estonia, 2018.
58. Barreau, J.-B.; Gaugne, R.; Olivier, A.-H.; Llinares, S.; Gouranton, V. Reconstitution de la vie à bord d'un navire de la Compagnie des Indes orientales au xviii^e siècle. *In Situ* **2020**. [[CrossRef](#)]
59. Barreau, J.-B.; Colleter, R. Virtualanthropy: Towards an Open-Source Tool for the Visualization of 2D Anthropology Images Positioned In 3D. *Open Access J. Arch. Anthropol.* **2020**, *2*, 3.
60. Betoux, J. *Les Terrassements: Première Partie (Suite)*; Revue Générale des Routes et des Aéroports: Paris, France, 1979.
61. Delfaut, A. Méthode d'évaluation Des Hauteurs de Montée d'un Fontis En Sol Meuble. *Bull. Lab. Ponts Chaussées* **2007**, *20*, 3–22.
62. Goujou, J.-C.; Debrand-Passard, S.; Hantzpergue, P.; Lebret, P. *Carte Géologique de La France à 1/50000, Notice de La Feuille des Sables d'Olonne/Longeville (584)*; Editions du BRGM: Orléans, France, 1994.
63. Huang, J.; Zhou, Y.; Niessner, M.; Shewchuk, J.R.; Guibas, L.J. QuadriFlow: A Scalable and Robust Method for Quadrangulation. *Comput. Graph. Forum* **2018**, *37*, 147–160. [[CrossRef](#)]
64. Schuh, A.; Dutailly, B.; Nogueira, D.C.; Santos, F.; Arensburg, B.; Vandermeersch, B.; Coqueugniot, H.; Tillier, A.-M. La Mandibule de l'adulte Qafzeh 25 (Paléolithique Moyen), Basse Galilée. Reconstruction Virtuelle 3D et Analyse Morphométrique. *Paléorient* **2017**, *43*, 49–59. [[CrossRef](#)]
65. Sabati, Z.; Bernik, A.; Jovanovska, D. 3D Modelling Functions and Algorithms. In Proceedings of the Central European Conference on Information and Intelligent Systems, Varazdin, Croatia, 22–24 September 2010; pp. 327–334.
66. Alexandre-Bidon, D. Images du cimetière chrétien au Moyen Age. In *Archéologie du Cimetière Chrétien—Actes du 2^e Colloque ARCHEA (Orléans, 29 septembre–1^{er} octobre 1994)*; Galinié, H., Zadora-Rio, E., Eds.; 11^e supplément à la Revue Archéologique de Centre de la France—Conseil Régional du Centre: Paris, France, 1996; pp. 79–93.
67. Rahtz, P. Grave Orientation. *Archaeol. J.* **1978**, *135*, 1–14. [[CrossRef](#)]
68. Blaizot, F. L'apport des méthodes de la paléo-anthropologie funéraire à l'interprétation des os en situation secondaire dans les nécropoles historiques—Problèmes relatifs au traitement et à l'interprétation des amas d'ossements. *Archéologie Médi Eacute Val.* **1996**, *26*, 1–22. [[CrossRef](#)]
69. Duday, H. Notes et Documents—Observations Ostéologiques et Décomposition Du Cadavre: Sépulture Colmatée Ou Espace Vide. *Rev. Archéologique Cent. Fr.* **1990**, *29*, 193–196. [[CrossRef](#)]
70. Salin, Édouard Les tombes gallo-romaines et mérovingiennes de la basilique de Saint-Denis (fouilles de janvier–février 1957). *Mémoires Inst. Natl. Fr.* **1960**, *44*, 169–264. [[CrossRef](#)]

71. Périn, P.; Calligaro, T.; Buchet, L.; Cassiman, J.J.; Darton, Y.; Gallien, V.; Poirot, J.P.; Rast, A.; Rücker, C.; Vallet, F. La Tombe d'Arégonde. Nouvelles analyses en laboratoire du mobilier métallique et des restes organiques de la défunte du sarcophage 49 de la basilique de Saint-Denis. *Antiq. Natl.* **2005**, *37*, 181–206.
72. Jouneau, D.; Colleter, R.; Gryspeirt, N.; Rolland, N.; Guillon, M. Mise en terre et mise en pierre dans le cimetière de Saint-Crespin: Diversité du sarcophage à Romilly-sur-Andelle (Eure). In *Les Sarcophages de l'Antiquité tardive et du haut Moyen Age: Fabrication, Utilisation, Diffusion*; Cartron, I., Henrion, F., Scullier, C., Eds.; Suppl. Aquitania: Bordeaux, France, 2015; Volume 34, pp. 361–378.
73. Deguilloux, M.; Pemonge, M.; Mendisco, F.; Thibon, D.; Cartron, I.; Castex, D. Ancient DNA and kinship analysis of human remains deposited in Merovingian necropolis sarcophagi (Jau Dignac et Loirac, France, 7th–8th century AD). *J. Archaeol. Sci.* **2014**, *41*, 399–405. [[CrossRef](#)]
74. Christaller, W. *Die zentralen Orte in Süddeutschland: Eine ökonomisch-geographische Untersuchung über die Gesetzmässigkeit der Verbreitung und Entwicklung der Siedlungen mit städtischen Funktionen*; Gustav Fischer: Jena, Germany, 1933.
75. Zadora-Rio, E.; Galinié, H. Les changements dans l'organisation spatiale du cimetière paroissial de Rigny, Indre-et-Loire, (XIe/XIIe—XIXe siècle). In *Archéologie du Cimetière Chrétien—Actes du 2e Colloque A.R.C.H.E.A. (Orléans, 29 septembre-1er octobre 1994)*; Galinié, H., Zadora-Rio, E., Eds.; 11e supplément à la Revue Archéologique de Centre de la France—Conseil Régional du Centre: Tours, France, 1996; pp. 172–182.
76. Boissavit-Camus, B.; Zadora-Rio, E. L'organisation spatiale des cimetières paroissiaux. In *Archéologie du Cimetière Chrétien—Actes du 2ème Colloque A.R.C.H.E.A. Orléans, 29 septembre-1er octobre 1994*; Galinié, H., Zadora-Rio, E., Eds.; 11e supplément à la Revue Archéologique de Centre de la France—Conseil Régional du Centre: Tours, France, 1996; pp. 49–53.
77. Ariès, P. *L'homme Devant La Mort*; Editions du Seuil: Paris, France, 1977.
78. Séguy, I.; Buchet, L.; Belaugues-Rossard, M.; Couvert, N.; Perraut, C.; Beurmier, P.; Bringé, A. Tables-Types de Mortalité Pour Les Populations Pré-Industrielles et Leurs Applications En Paléodémographie. In *Proceedings of the XXVe Congrès International de la Population de l'UIESP, Tours, France, 18–23 July 2005*; pp. 1–17.
79. Castex, D. Identification and Interpretation of Historical Cemeteries Linked to Epidemics. In *Paleomicrobiology: Past Human Infections*; Raoult, D., Drancourt, M., Eds.; Springer: Berlin/Heidelberg, Germany, 2008; pp. 23–48. ISBN 978-3-540-75855-6.
80. Ligou, D. L'Évolution Des Cimetières. *Arch. Sci. Soc. Relig.* **1975**, *20*, 61–77. [[CrossRef](#)]
81. Treffort, C. *L'Eglise Carolingienne et la Mort: Christianisme, Rites Funéraires et Pratiques Commémoratives*; Collection d'Histoire et d'Archéologie Médiévales; Presses Universitaires de Lyon: Lyon, France, 1996; ISBN 2-7297-0558-9.
82. Colleter, R.; Le Boulanger, F.; Pichot, D. *Église, Cimetière et Paroissiens. Bréal-sous-Vitré (Ille-et-Vilaine), Etude Historique, Archéologique et Anthropologique (VIIe–XVIIIe siècle)*; Archéologie Aujourd'hui; Errance: Paris, France, 2012; ISBN 978-2-87772-490-6.
83. Melilli, V. Sepulture in Chiesa e sub Stillicidio in età Medievale. La Toscana Settentrionale (V–XV secolo). Ph.D. Thesis, Università di Pisa, Pisa, Italy, 2019.
84. Colleter, R. *Les Cimetières Mérovingiens en Mayenne (VIe—VIIe siècle) La Mayenne: Archéologie, Histoire Suppl*; Soc. d'Archéologie et d'Histoire de la Mayenne: Laval, France, 2003; ISBN 978-2-913201-03-3.
85. Urlacher, J.-P.; Passard-Urlacher, F.; Gizard, S. *Saint-Vit Les Champs Traversains—Doubs—Nécropole Mérovingienne, VIe–VIIe Siècle Ap. J.-C. et Enclos Protohistorique, IXe–Ve Siècle Av.J.-C.*; Presses Universitaires de Franche-Comté: Besançon, France, 2009.
86. Legoux, R. *La Nécropole Mérovingienne de Bulles (Oise)*; Mémoires de l'Association Française d'archéologie Mérovingienne: Saint-Germain-en-Laye, France, 2011; Volume 2, ISBN 978-2-9524032-9-0.
87. Fletcher, R. Some spatial analyses of Chalcolithic settlement in Southern Israel. *J. Archaeol. Sci.* **2008**, *35*, 2048–2058. [[CrossRef](#)]
88. Carrer, F. Interpreting Intra-site Spatial Patterns in Seasonal Contexts: An Ethnoarchaeological Case Study from the Western Alps. *J. Archaeol. Method Theory* **2015**, *24*, 303–327. [[CrossRef](#)] [[PubMed](#)]
89. Bachagha, N.; Wang, X.; Luo, L.; Li, L.; Khatteli, H.; Lasaponara, R. Remote sensing and GIS techniques for reconstructing the military fort system on the Roman boundary (Tunisian section) and identifying archaeological sites. *Remote Sens. Environ.* **2020**, *236*, 111418. [[CrossRef](#)]
90. Carrer, F.; Kossowski, T.M.; Wilk, J.; Pietrzak, M.B.; Bivand, R.S. The application of Local Indicators for Categorical Data (LICD) to explore spatial dependence in archaeological spaces. *J. Archaeol. Sci.* **2021**, *126*, 105306. [[CrossRef](#)]
91. Tobler, W.R. A Computer Movie Simulating Urban Growth in the Detroit Region. *Econ. Geogr.* **1970**, *46*, 234. [[CrossRef](#)]
92. Anselin, L. *Spatial Econometrics: Methods and Models*; Kluwer Academic Publishers: Boston, MA, USA, 1988.
93. Getis, A. A History of the Concept of Spatial Autocorrelation: A Geographer's Perspective. *Geogr. Anal.* **2008**, *40*, 297–309. [[CrossRef](#)]
94. Turner, S. Historic Landscape Characterisation: A landscape archaeology for research, management and planning. *Landsc. Res.* **2006**, *31*, 385–398. [[CrossRef](#)]
95. Herring, P.C. Framing Perceptions of the Historic Landscape: Historic Landscape Characterisation (HLC) and Historic Land-Use Assessment (HLA). *Scott. Geogr. J.* **2009**, *125*, 61–77. [[CrossRef](#)]
96. Medyńska-Gulij, B.; Zagata, K. Experts and Gamers on Immersion into Reconstructed Strongholds. *ISPRS Int. J. Geo-Inform.* **2020**, *9*, 655. [[CrossRef](#)]
97. Büyüksalih, G.; Kan, T.; Özkan, G.E.; Meriç, M.; Isın, L.; Kersten, T.P. Preserving the Knowledge of the Past Through Virtual Visits: From 3D Laser Scanning to Virtual Reality Visualisation at the Istanbul Çatalca İnceğiz Caves. *PFGJ. Photogramm. Remote Sens. Geoinform. Sci.* **2020**, *88*, 133–146. [[CrossRef](#)]

98. Barreau, J.-B.; Gagne, R.; Bernard, Y.; Le Cloirec, G.; Gouranton, V. Virtual reality tools for the west digital conservatory of archaeological heritage. In Proceedings of the Proceedings of the 2014 Virtual Reality International Conference ACM, Laval, France, 9–11 April 2014; pp. 1–4.
99. Barreau, J.-B. Techniques de Production, d'Exploration et d'Analyse d'Environnements Archéologiques Virtuels. Ph.D. Thesis, INSA, Rennes, France, 2017.
100. Memmi, D. Le corps mort dans l'histoire des sensibilités. *Communications* **2015**, *97*, 131–145.
101. Colleter, R.; Adèle, P.-A. Les restes humains archéologiques en France: Entre objets de science et sujets de droit. *Can. J. Bioeth.* **2019**, *2*, 97–108. [[CrossRef](#)]
102. Remondino, F. Heritage Recording and 3D Modeling with Photogrammetry and 3D Scanning. *Remote Sens.* **2011**, *3*, 1104–1138. [[CrossRef](#)]
103. Barsanti, S.G.; Remondino, F.; Visintini, D. 3D Surveying and Modeling of Archaeological Sites—Some Critical Issues. *ISPRS Ann. Photogramm. Remote. Sens. Spat. Inf. Sci.* **2013**, *II-5/W1*, 145–150. [[CrossRef](#)]
104. Colleter, R.; Dabernat, H.; Aubert, G.; Duchesne, S.; Dedouit, F.; Mokrane, F.-Z.; Telmon, N.; Crubézy, É. Avec ou sans hypothèse? Qu'attendre de la paléoépidémiologie? Exemple à partir de l'étude d'un couvent breton des ordres mendiants. In *Archéologie de La Santé, Anthropologie Du Soins, (La Découverte, Inrap)*; La Découverte: Paris, France, 2019; pp. 145–158.